Research in Physics 2008-2013

Theoretical Physics 1
Condensed Matter, Materials and Soft Matter Physics 38
- Nanoscale Physics Cluster 38
- Magnetic Resonance Cluster 96
- Materials Physics Cluster 121

Astronomy and Astrophysics (A&A) 172
Elementary Particle Physics (EPP) 204
Centre for Fusion Space and Astrophysics (CFSA) 247

Elementary Particle Physics (EPP)

- *9 Staff; 11 PDRAs; 17 PhDs;*
- *688 articles; 11,126 citations; £7.1 M grant awards; >£12 M in-kind; 10 PhDs awarded*

With the Large Hadron Collider (LHC) at CERN now producing scientific results on a broad front, including constraining the Higgs boson, with its luminosity projected to increase significantly, and with a proliferation of new international opportunities in neutrino physics, elementary particle physics is enjoying a particularly fertile period. The EPP Group is fully involved in this international search for new physical phenomena, participating in particle physics experiments judged to have the highest likelihood of success. Since 2008, EPP has considerably broadened its scope, from neutrinos and heavy quarks at the luminosity frontier, to now include discovery searches at the energy frontier. The highly-regarded group has rapidly grown from being the smallest and newest UK EPP group in 2008, to a secure position with STFC rolling/consolidated grants (2009 & 2012).

In the early part of the period, significant physics was extracted from existing data sets, BaBar, Belle, & CDF, whilst strongly contributing to building the **T2K** neutrino experiment in Japan (**Barker**, **Boyd**) and joining the **LHCb** beauty quark experiment at CERN (**Gershon**, **Kreps, Blake**). The T2K investment paid off with the first indication for $\nu_\mu \rightarrow \nu_e$ conversions in 2011. Since 2011 the EPP Group has diversified its portfolio by taking a significant role in **ATLAS** at CERN (**Farrington, Harrison, Murray**), culminating in the successful discovery of a new Higgs-like boson in 2012. A priority for the group is to take leadership roles where possible – currently Warwick provides the Physics Coordinators for two of the four major CERN experiments: ATLAS (**Murray**) and LHCb (**Gershon**). The neutrino focus has also been consolidated by joining **SuperNEMO**, a double beta decay experiment in France with two future phases. This now positions the EPP Group in four primary international particle physics experiments, which should ensure both an exciting scientific future and an even stronger funding base. Subsidiary activities in detector research, flavour phenomenology and new initiatives towards the NuSTORM, LBNE and Hyper-K experiments, together with ATLAS and LHCb upgrades will develop the group's longer term programme.

Characterization and Simulation of the Response of Multi Pixel Photon Counters to Low Light Levels

Nucl. Instrum. Meth. A 656 (2011) 69-83 http://dx.doi.org/10.1016/j.nima.2011.07.022

T2K Collaboration; A. Vacheret, G.J. Barker et al.

The calorimeter, range detector and active target elements of the T2K near detectors rely on the Hamamatsu Photonics Multi-Pixel Photon Counters (MPPCs) to detect scintillation light produced by charged particles. Detailed measurements of the MPPC gain, afterpulsing, crosstalk, dark noise, and photon detection efficiency for low light levels are reported. In order to account for the impact of the MPPC behavior on T2K physics observables, a simulation program has been developed based on these measurements. The simulation is used to predict the energy resolution of the detector.

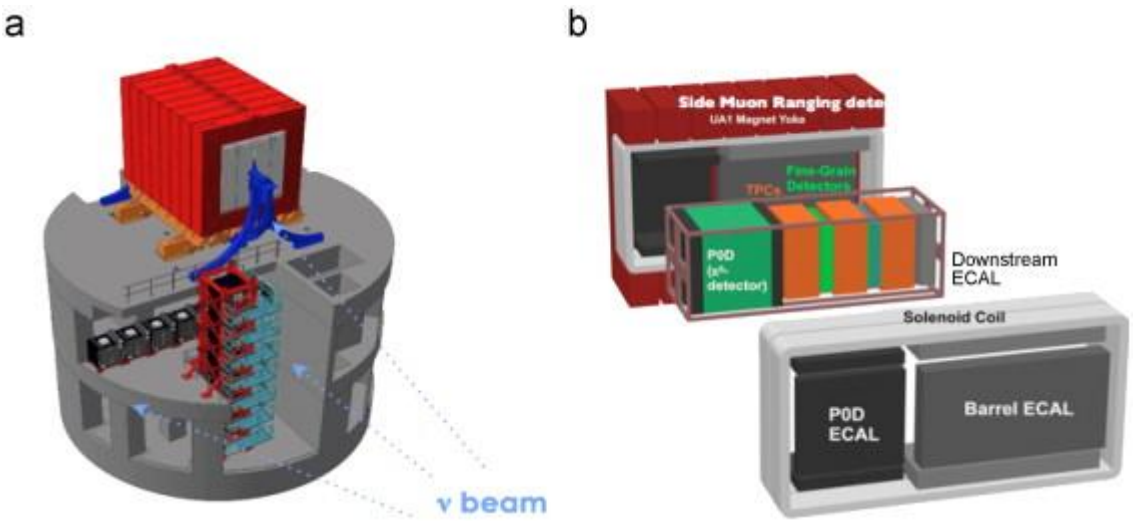

Schematic view of (a) the T2K ND280 near detector complex consisting of the on-axis neutrino beam monitor (the “cross” configuration of cubical black modules on the two lower levels) and off-axis near neutrino detector on the top level, and (b) an exploded view of the off-axis near neutrino detector.

The T2K Experiment

Nucl. Instrum. Meth. A659 (2011) 106-135 doi:10.1016/j.nima.2011.06.067

T2K Collaboration, incl. G Barker, S. Boyd, P.F. Harrison

The T2K experiment is a long baseline neutrino oscillation experiment. Its main goal is to measure the last unknown lepton sector mixing angle θ_{13}θ13 by observing ν_eνe appearance in a ν_μνμ beam. It also aims to make a precision measurement of the known oscillation parameters, Δm^2_{23}Δm232 and $\sin^2 2\theta_{23}$sin22θ23, via ν_μνμ disappearance studies. Other goals of the experiment include various neutrino cross-section measurements and sterile neutrino searches. The experiment uses an intense proton beam generated by the J-PARC accelerator in Tokai, Japan, and is composed of a neutrino beamline, a near detector complex (ND280), and a far detector (Super-Kamiokande) located 295 km away from J-PARC. This paper provides a comprehensive review of the instrumentation aspect of the T2K experiment and a summary of the vital information for each subsystem.

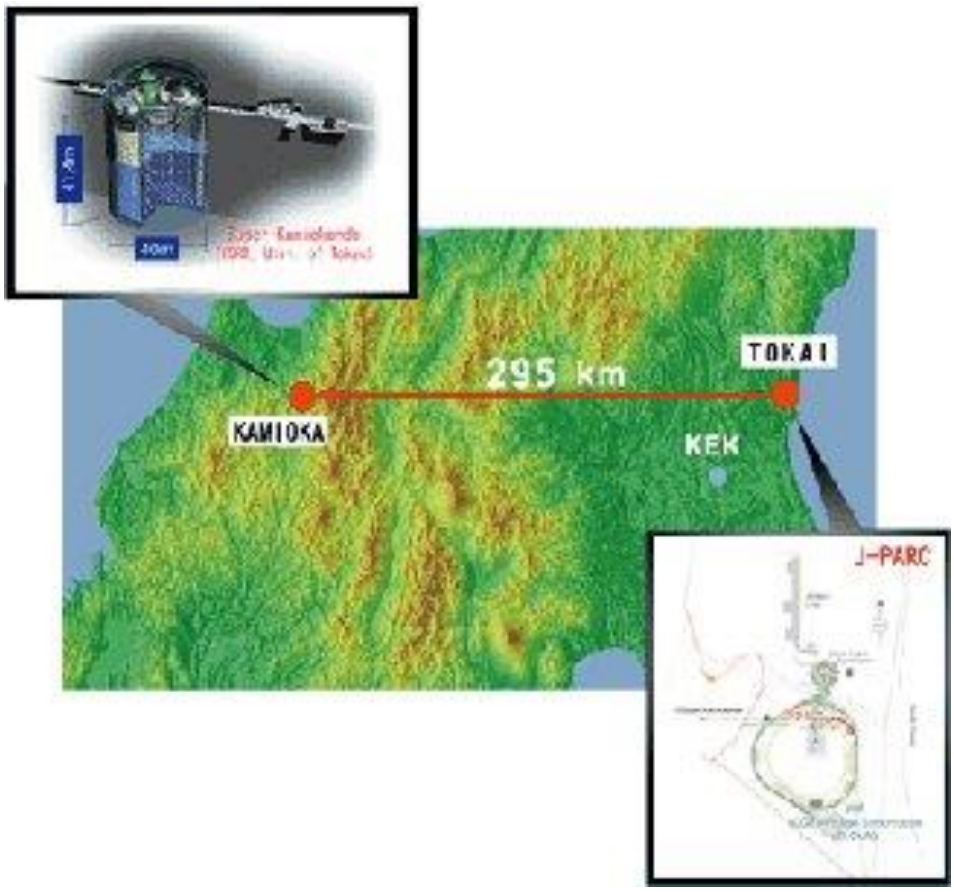

Indication of Electron Neutrino Appearance from an Accelerator-produced Off-axis Muon Neutrino Beam.

Phys.Rev.Lett. 107 (2011) 041801 DOI: http://dx.doi.org/10.1103/PhysRevLett.107.041801

T2K Collaboration, incl. G Barker, S. Boyd, P.F. Harrison

The T2K experiment observes indications of $\nu_\mu \rightarrow \nu e$ appearance in data accumulated with 1.43×10^{20} protons on target. Six events pass all selection criteria at the far detector. In a three-flavor neutrino oscillation scenario with $|\Delta m^2_{23}|=2.4\times10^{-3}$ eV^2, $\sin^2 2\theta_{23}=1$ and $\sin^2 2\theta_{13}=0$, the expected number of such events is 1.5 ± 0.3(syst). Under this hypothesis, the probability to observe six or more candidate events is 7×10^{-3}, equivalent to 2.5σ significance. At 90% C.L., the data are consistent with $0.03(0.04)<\sin^2 2\theta_{13}<0.28(0.34)$ for $\delta CP=0$ and a normal (inverted) hierarchy.

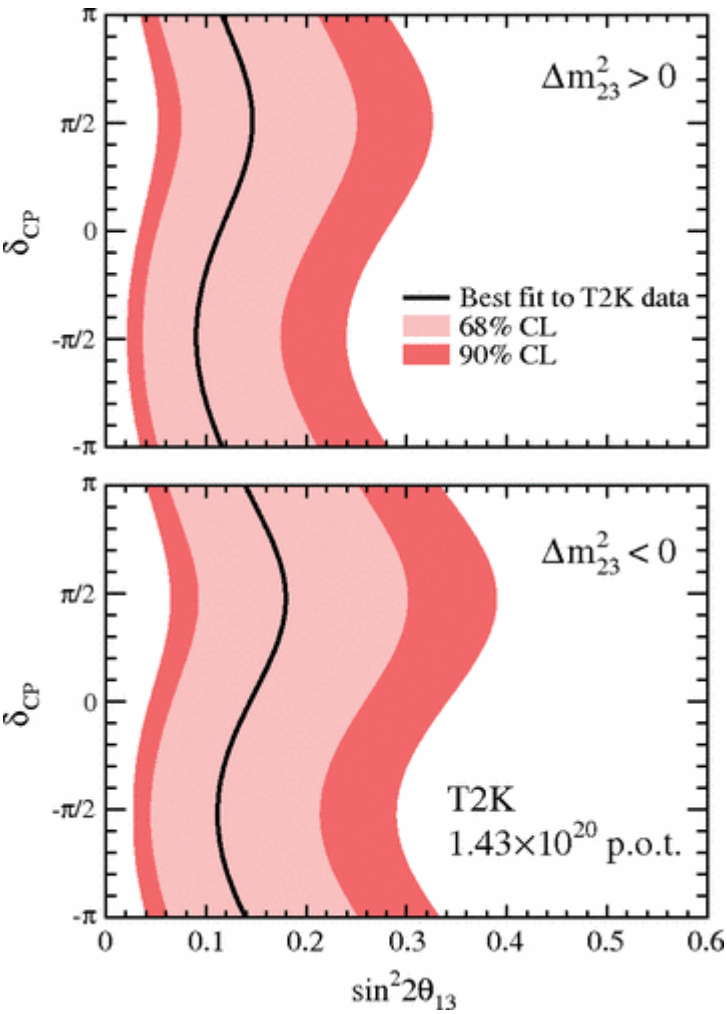

The 68% and 90% C.L. regions for $\sin^2 2\vartheta_{13}$ for each value of δ_{CP}, consistent with the observed number of events in the three-flavor oscillation case for normal (top) and inverted (bottom) mass hierarchy. The other oscillation parameters are fixed (see text). The best fit values are shown with solid lines.

First muon-neutrino disappearance study with an off-axis beam

Physical Review D 85, 031103(R) (2012) DOI: http://dx.doi.org/10.1103/PhysRevD.85.031103

T2K Collaboration, incl. G Barker, S. Boyd, P.F. Harrison

We report a measurement of muon-neutrino disappearance in the T2K experiment. The 295-km muon-neutrino beam from Tokai to Kamioka is the first implementation of the off-axis technique in a long-baseline neutrino oscillation experiment. With data corresponding to 1.43×10^{20} protons on target, we observe 31 fully-contained single μ-like ring events in Super-Kamiokande, compared with an expectation of 104 ± 14 (syst) events without neutrino oscillations. The best-fit point for two-flavor $\nu\mu\rightarrow\nu\tau$ oscillations is $\sin^2(2\theta_{23})=0.98$ and $|\Delta m^2_{32}|=2.65\times10^{-3}$ eV2. The boundary of the 90% confidence region includes the points $(\sin^2(2\theta_{23}),|\Delta m^2_{32}|)=(1.0, 3.1\times10^{-3}\ \mathrm{eV}^2)$, $(0.84, 2.65\times10^{-3}\ \mathrm{eV}^2)$ and $(1.0, 2.2\times10^{-3}\ \mathrm{eV}^2)$.

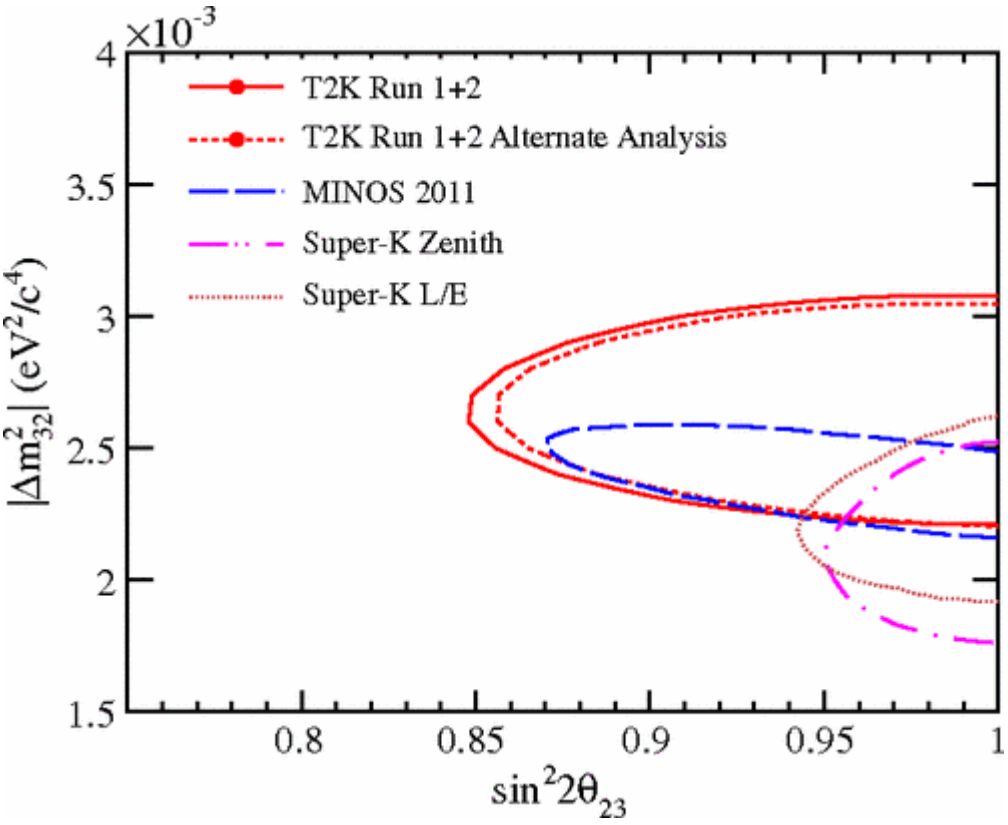

The 90% confidence regions for $\sin^2(2\vartheta_{23})$ and $|\Delta m_{32}{}^2|$; results from the two analyses reported here are compared with those from MINOS [5] and Super-Kamiokande [6, 31].

Measurement of the Inclusive NuMu Charged Current Cross section on Carbon in the Near detector of the T2K Experiment

Phys. Rev. D 87, 092003 (2013) DOI: http://dx.doi.org/10.1103/PhysRevD.87.092003

T2K Collaboration, incl. G Barker, S. Boyd, P.F. Harrison

T2K has performed the first measurement of $\nu\mu$ inclusive charged current interactions on carbon at neutrino energies of ~1 GeV where the measurement is reported as a flux-averaged double differential cross section in muon momentum and angle. The flux is predicted by the beam Monte Carlo and external data, including the results from the NA61/SHINE experiment. The data used for this measurement were taken in 2010 and 2011, with a total of 10.8×10^{19} protons-on-target. The analysis is performed on 4485 inclusive charged current interaction candidates selected in the most upstream fine-grained scintillator detector of the near detector. The flux-averaged total cross section is $\langle\sigma_{CC}\rangle_{\phi}=(6.91\pm0.13(\text{stat})\pm0.84(\text{syst}))\times10^{-39}$ cm^2/nucleon for a mean neutrino energy of 0.85 GeV.

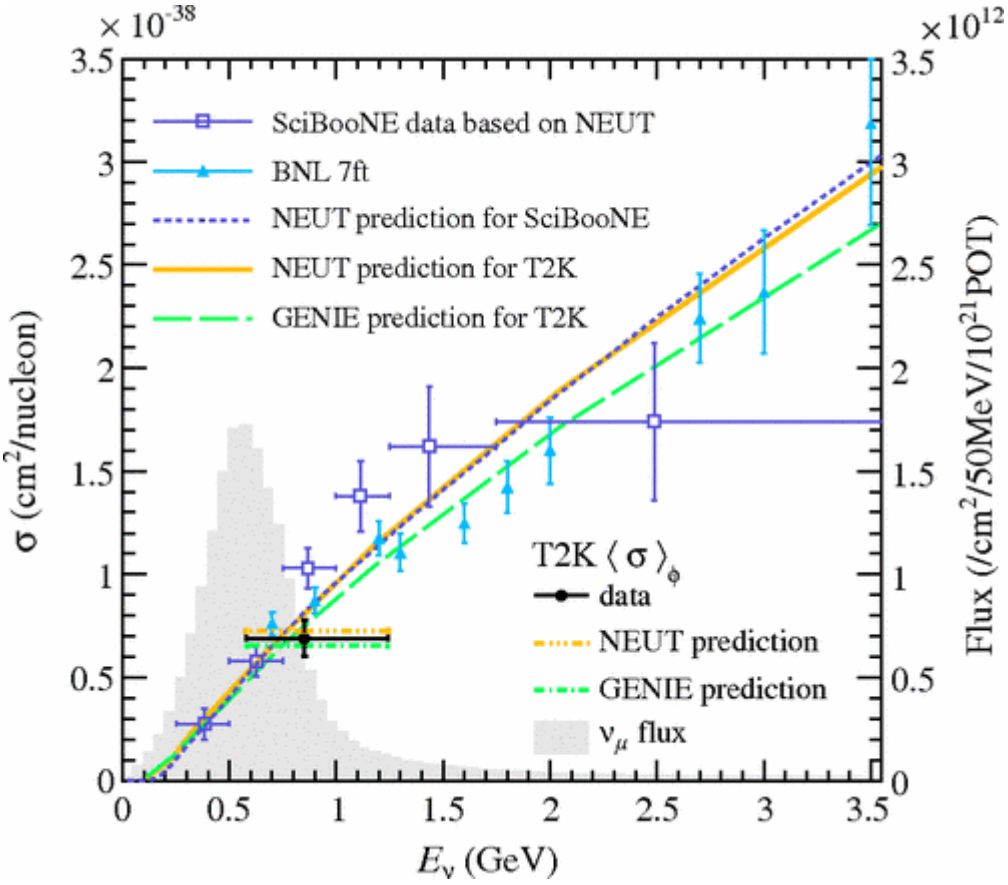

The T2K total flux-averaged cross section with the NEUT and the GENIE prediction for T2K and SciBooNE. The T2K data point is placed at the flux mean energy. The vertical error represents the total (statistical and systematic) uncertainty, and the horizontal bar represent 68% of the flux at each side of the mean energy. The T2K flux distribution is shown in grey. The predictions for SciBooNE have been done for a C_8H_8 target which is comparable to the mixed T2K target. BNL data has been measured on deuterium.

Evidence of electron neutrino appearance in a muon beam

Phys. Rev. D 88, 032002 (2013) DOI: http://dx.doi.org/10.1103/PhysRevD.88.032002

T2K Collaboration, incl. G Barker, S. Boyd, P.F. Harrison

The T2K Collaboration reports evidence for electron neutrino appearance at the atmospheric mass splitting, $|\Delta m^2_{32}| \approx 2.4\times10^{-3}$ eV^2. An excess of electron neutrino interactions over background is observed from a muon neutrino beam with a peak energy of 0.6 GeV at the Super-Kamiokande (SK) detector 295 km from the beam's origin. Signal and background predictions are constrained by data from near detectors located 280 m from the neutrino production target. We observe 11 electron neutrino candidate events at the SK detector when a background of 3.3 ± 0.4(syst) events is expected. The background-only hypothesis is rejected with a p value of 0.0009 (3.1σ), and a fit assuming $\nu_\mu \rightarrow \nu_e$ oscillations with $\sin^2 2\theta_{23}=1$, $\delta CP=0$ and $|\Delta m^2_{32}|=2.4\times10^{-3}$ eV^2 yields $\sin^2 2\theta_{13}=0.088^{+0.049}_{-0.039}$(stat+syst).

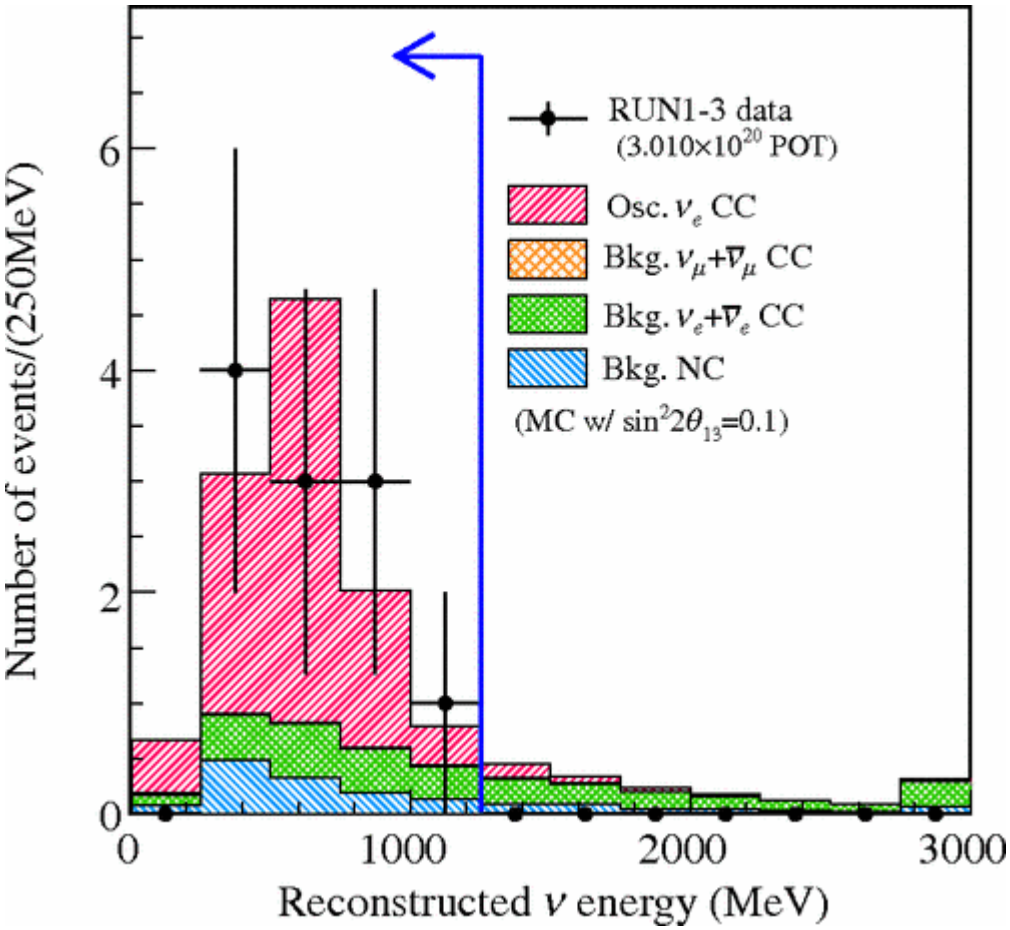

Distribution of the reconstructed neutrino energy spectrum of the events which pass all ν_e appearance signal selection criteria with the exception of the energy cut. The data are shown as points with error bars (statistical only) and the MC predictions are in shaded histograms. The arrow shows the selection criterion $E_\nu^{rec}<1250$ MeV.

A study of quasi-elastic muon neutrino and antineutrino scattering in the NOMAD experiment.

Eur.Phys.J. C63 (2009) 355-381 http://dx.doi.org/10.1140/epjc/s10052-009-1113-0

NOMAD Collaboration, incl. S. Boyd

We have studied the muon neutrino and antineutrino quasi-elastic (QEL) scattering reactions ($\nu_\mu n \to \mu^- p$ and $\bar{\nu}_\mu p \to \mu^+ n$) using a set of experimental data collected by the NOMAD Collaboration. We have performed measurements of the cross-section of these processes on a nuclear target (mainly carbon) normalizing it to the total ν_μ ($\bar{\nu}_\mu$) charged-current cross section. The results for the flux-averaged QEL cross sections in the (anti)neutrino energy interval 3–100 GeV are $\langle\sigma_{\rm qel}\rangle_{\nu\mu}=(0.92\pm0.02({\rm stat})\pm0.06({\rm syst}))\times10^{-38}$ cm^2 and $\langle\sigma_{\rm qel}\rangle_{\nu^-\mu}=(0.81\pm0.05({\rm stat})\pm0.09({\rm syst}))\times10^{-38}$ cm^2 for neutrino and antineutrino, respectively. The axial mass parameter M_A was extracted from the measured quasi-elastic neutrino cross section. The corresponding result is M_A =1.05±0.02(stat)±0.06(syst) GeV. It is consistent with the axial mass values recalculated from the antineutrino cross section and extracted from the pure Q^2 shape analysis of the high purity sample of ν_μ quasi-elastic 2-track events, but has smaller systematic error and should be quoted as the main result of this work. Our measured M_A is found to be in good agreement with the world average value obtained in previous deuterium filled bubble chamber experiments. The NOMAD measurement of M_A is lower than those recently published by K2K and MiniBooNE Collaborations. However, within the large errors quoted by these experiments on M_A, these results are compatible with the more precise NOMAD value.

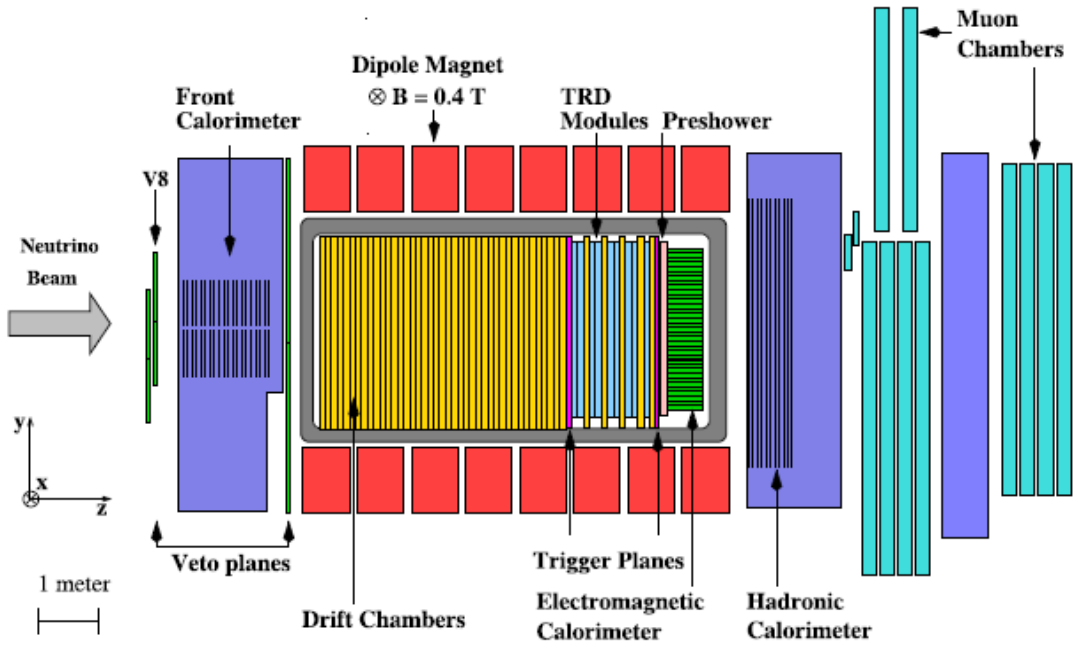

A side-view of the NOMAD detector

Measurement of Muon Neutrino Quasi-Elastic Scattering on a Hydrocarbon Target at Eν~3.5 GeV

Phys.Rev.Lett. 111, 022502 (2013) 10.1103/PhysRevLett.111.022501

MINERvA Collaboration incl. S. Boyd

We have isolated $\bar{\nu}_\mu$ charged-current quasielastic (QE) interactions occurring in the segmented scintillator tracking region of the MINERvA detector running in the NuMI neutrino beam at Fermilab. We measure the flux-averaged differential cross section, $d\sigma/dQ^2$, and compare to several theoretical models of QE scattering. Good agreement is obtained with a model where the nucleon axial mass, M_A, is set to $0.99\ \mathrm{GeV}/c^2$ but the nucleon vector form factors are modified to account for the observed enhancement, relative to the free nucleon case, of the cross section for the exchange of transversely polarized photons in electron-nucleus scattering. Our data at higher Q^2 favor this interpretation over an alternative in which the axial mass is increased.

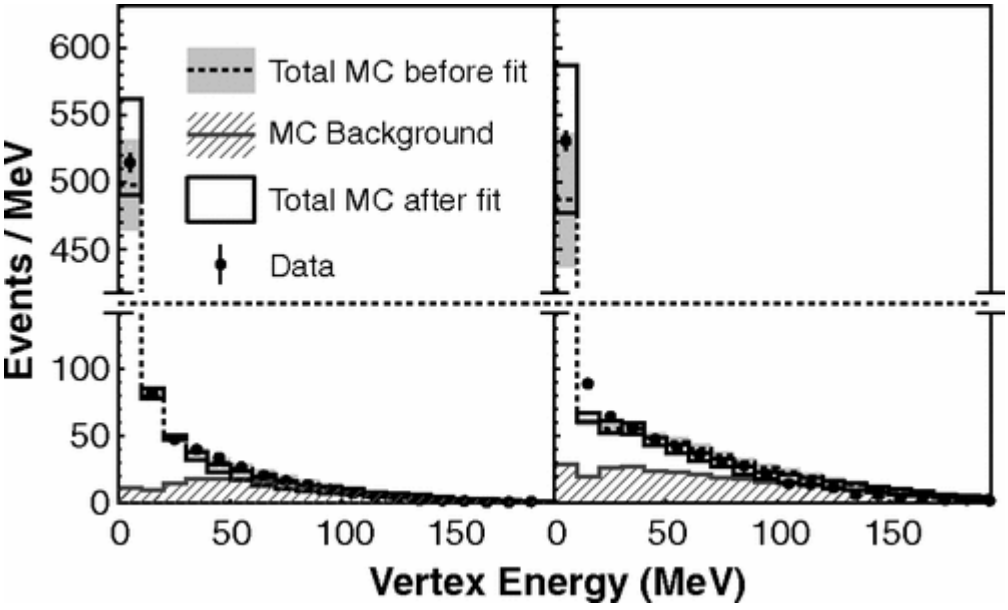

Reconstructed vertex energy of events passing the selection criteria compared to the GENIE RFG model for $Q_{QE}^2<0.2\ \mathrm{GeV}^2/c^2$ (left) and for $Q_{QE}^2>0.2\ \mathrm{GeV}^2/c^2$ (right).

Characterisation of a silicon photomultiplier device for applications in liquid argon based neutrino physics and dark matter searches

JINST 3, P10001 (2008) http://dx.doi.org/10.1088/1748-0221/3/10/P10001

Lightfoot, PK, Barker, GJ, Mavrokoridis, K, Ramachers, YA, Spooner, NJC

The performance of a silicon photomultiplier has been assessed at low temperature in order to evaluate its suitability as a scintillation readout device in liquid argon particle physics detectors. The gain, measured as 2.1×10^6 for a constant over-voltage of 4V was measured between 25°C and -196°C and found to be invariant with temperature, the corresponding single photoelectron dark count rate reducing from 1MHz to 40Hz respectively. Following multiple thermal cycles no deterioration in the device performance was observed. The photon detection efficiency (PDE) was assessed as a function of photon wavelength and temperature. For an over-voltage of 4V, the PDE, found again to be invariant with temperature, was measured as 25% for 460nm photons and 11% for 680nm photons. Device saturation due to high photon flux rate, observed both at room temperature and -196°C, was again found to be independent of temperature. Although the output signal remained proportional to the input signal so long as the saturation limit was not exceeded, the photoelectron pulse resolution and decay time increased slightly at −196°C.

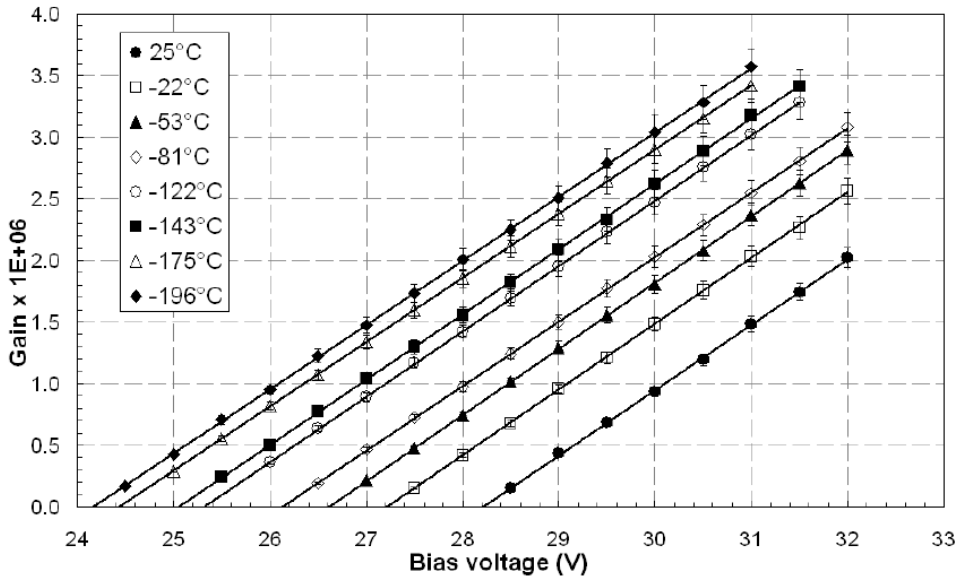

Dependency of the gain on the bias voltage for a range of device temperatures.

Optical readout tracking detector concept using secondary scintillation from liquid argon generated by a thick gas electron multiplier

JINST 4, P04002 (2009) doi:10.1088/1748-0221/4/04/P04002

Lightfoot, PK, Barker, GJ, Mavrokoridis, K, Ramachers, YA, Spooner, NJC

For the first time secondary scintillation, generated within the holes of a thick gas electron multiplier (THGEM) immersed in liquid argon, has been observed and measured using a silicon photomultiplier device (SiPM). 250 electron-ion pairs, generated in liquid argon via the interaction of a 5.9 keV Fe-55 gamma source, were drifted under the influence of a 2.5 kV/cm field towards a 1.5 mm thickness THGEM, the local field sufficiently high to generate secondary scintillation light within the liquid as the charge traversed the central region of the THGEM hole. The resulting VUV light was incident on an immersed SiPM device coated in the waveshifter tetraphenyl butadiene (TPB), the emission spectrum peaked at 460 nm in the high quantum efficiency region of the device. For a SiPM over-voltage of 1 V, a THGEM voltage of 9.91 kV, and a drift field of 2.5 kV/cm, a total of 62±20 photoelectrons were produced at the SiPM device per Fe-55 event, corresponding to an estimated gain of 150±66 photoelectrons per drifted electron.

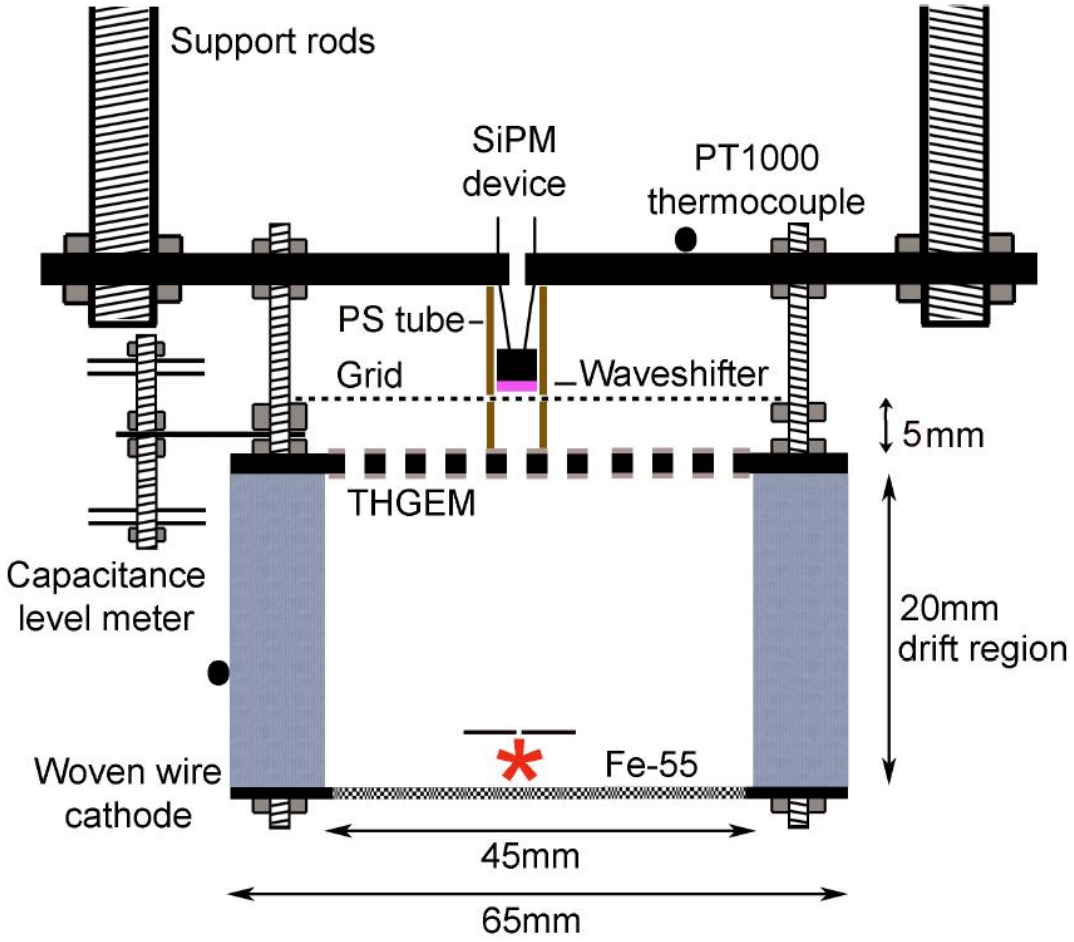

Internal assembly used to detect secondary scintillation in liquid argon.

Modelling electroluminescence in liquid argon

JINST 5, P10005 (2010) doi:10.1088/1748-0221/5/10/P10005

Stewart, DY, Barker, GJ, Bennieston, AJ, Harrison, PF, Lightfoot, PK, McConkey, N, Morgan, B, Ramachers, YA, Robinson, M, Spooner, NJC, Thompson, L

We present Monte-Carlo simulations of electron transport through liquid argon motivated by our recent observation of electroluminescence light emanating from a thick gaseous electron multiplier (THGEM) in a liquid argon volume. All known elastic and inelastic reaction cross-sections have been accounted for, providing electroluminescence light yield predictions for arbitrary electrostatic fields. This study concludes that the large field gradients needed to produce electroluminescence cannot be accounted for by straightforward electrostatic field calculations based on ideal THGEM holes, suggesting that further experimental investigations are required.

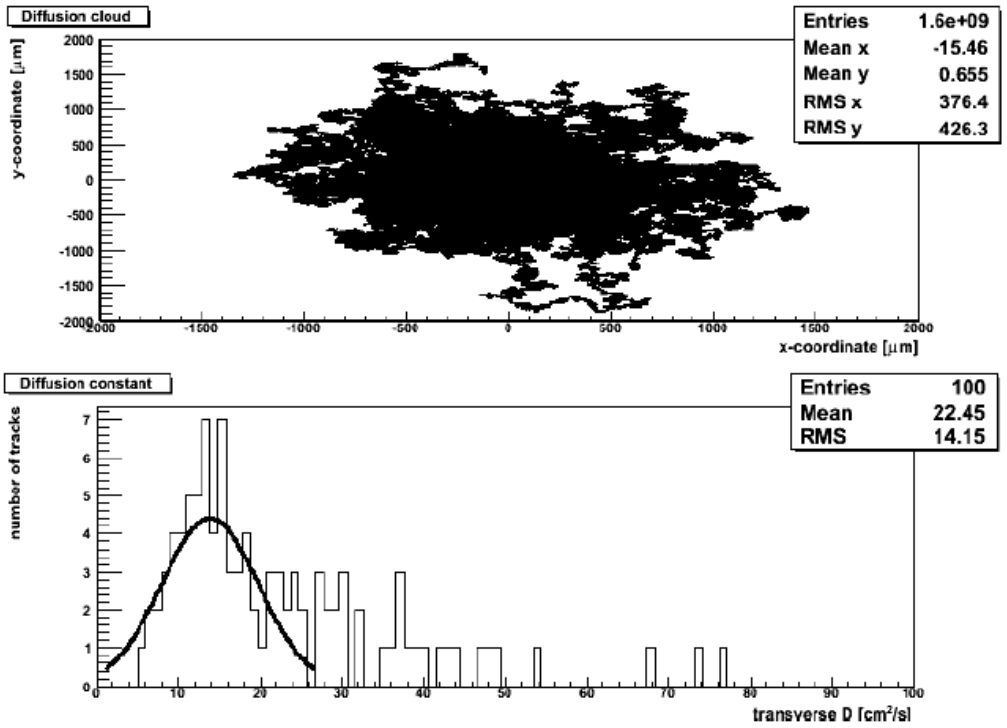

The upper panel shows the diffusion cloud of 100 individually simulated electrons after drifting through liquid argon in a drift field of 2 kV/cm. The statistical measures of the cloud are indicated in the insert, such as the RMS values and the slightly off-centre mean values. Taking this ensemble of electrons for transverse diffusion constant calculations results in a value of 71 cm^2/s as discussed in the text (the number of entries reflects the summing of 100 histograms on a 4000 x 4000 bin histogram, not the total of $2x10^{11}$ collision events displayed in it). The lower panel shows the histogram of individually calculated transverse diffusion constants for each simulated electron. About two thirds of electrons form a Gaussian peak of diffusion constant values at (13.9 x 6.0) cm^2/s, the rest displaying significantly higher diffusion constant values, presumably due to still correlated motion.

Electron-Hadron shower discrimination in a liquid argon time projection chamber

Euro Phys J C **73**: 2369 (2013) http://dx.doi.org/10.1140/epjc/s10052-013-2369-y

J.J. Back, G.J. Barker, A.J. Bennieston, S.B. Boyd, B. Morgan, and Y.A. Ramachers

By exploiting structural differences between electromagnetic and hadronic showers in a multivariate analysis we present an efficient Electron-Hadron discrimination algorithm for liquid argon time projection chambers, validated using Geant4 simulated data.

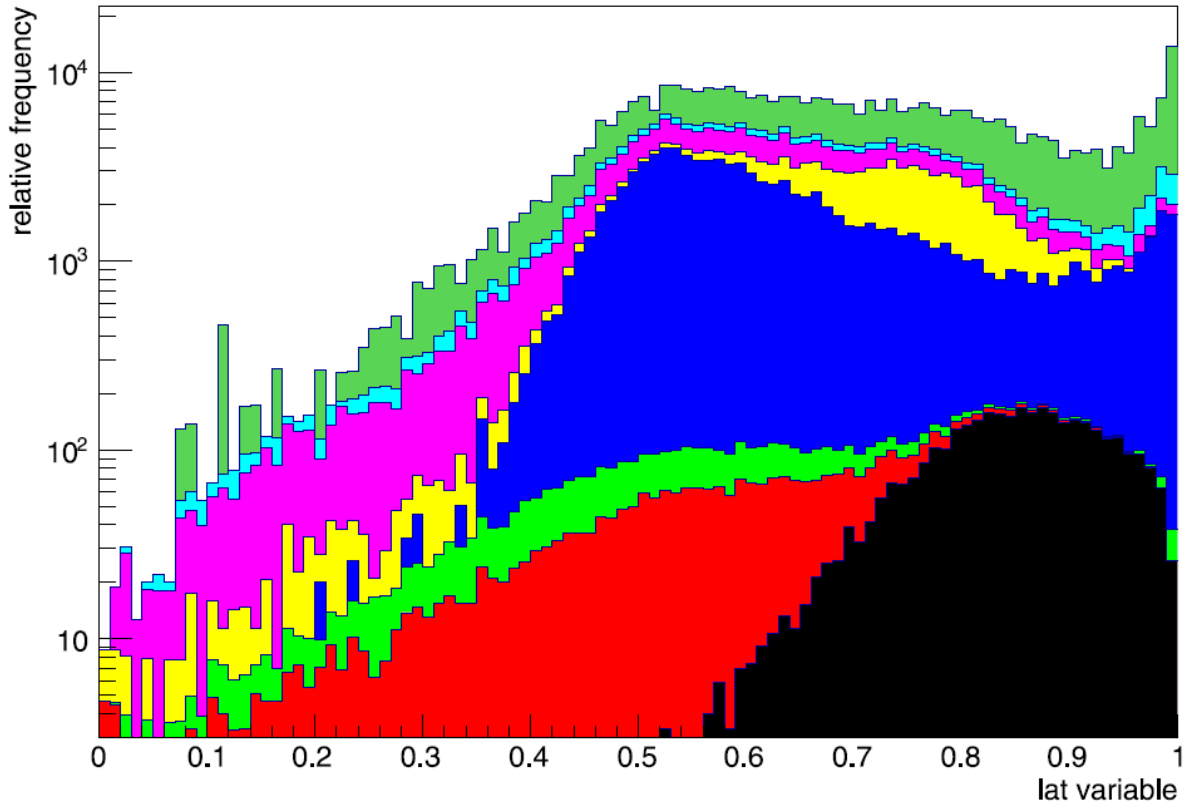

Stacked histogram example displaying the background composition due to simulated final state particles from the CN2PY neutrino beam case. This example shows the background in the 'lat' variable for an electron signal for the dominant anti-muon neutrino flavour

The Matrix of Unitarity Triangle Angles for Quarks

Phys. Lett. B 680, 328, (2009) doi:10.1016/j.physletb.2009.09.004

P.F.Harrison, S.Dallison and W.G.Scott

In the context of quark (as for lepton) mixing, we introduce the concept of the matrix of unitarity triangle angles Φ , emphasising that it carries equivalent information to the complex mixing matrix V itself. The angle matrix Φ has the added advantage, with respect to V , of being both basis- and phase-convention independent and consequently observable (indeed several Φ -matrix entries, e.g., $\Phi_{cs}=\alpha\Phi cs=\alpha$, $\Phi_{us}=\beta\Phi us=\beta$, etc. are already long-studied as directly measurable/measured in *B*-physics experiments). We give complete translation formulae between the mixing-matrix and angle-matrix representations. We go on to consider briefly the present state of the experimental data on the full angle matrix and some of the prospects for the future, with reference to both the quark and lepton cases.

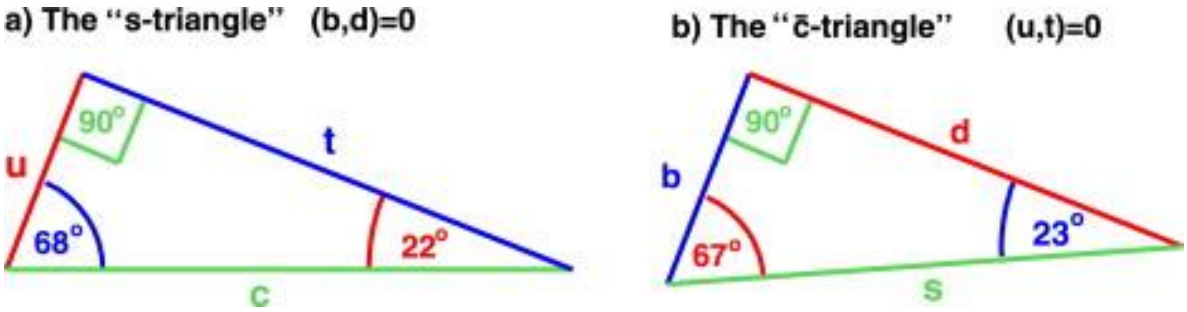

The indexing of unitarity triangles and their angles: (a) The familiar row-based (b ,d) = :s -triangle and (b) the closely similar $(u,t) =: \bar{c}$ (u,t)=:c¯-triangle.

Simplest Neutrino Mixing from S4 Symmetry

JHEP 1304 (2013) 087 DOI: 10.1007/JHEP04(2013)087

R. Krishnan, P.F. Harrison, W.G. Scott

In 2004, two of us proposed a texture, the "Simplest" neutrino mass matrix, which predicted sin(theta13)=sqrt((2 Solar-Delta m^2)/(3 Atm-Delta m^2)) and delta_CP=90 degrees. Using today's measured values for neutrino mass-squared differences, this prediction gives sin^2(theta13)~0.086+0.003-0.006, compared with a measured value, found by averaging the results of the Daya Bay and RENO experiments, of sin^2(theta13)=0.093+0.010-0.010. Here we present a specific model based on S4 symmetry leading to this successful texture in the context of the type-1 see-saw mechanism, assuming Majorana neutrinos. In this case, slightly different predictions are obtained relating theta13 to the light neutrino masses, which are in accord with current experimental limits and testable at future experiments. Large CP asymmetries remain a generic prediction of the texture.

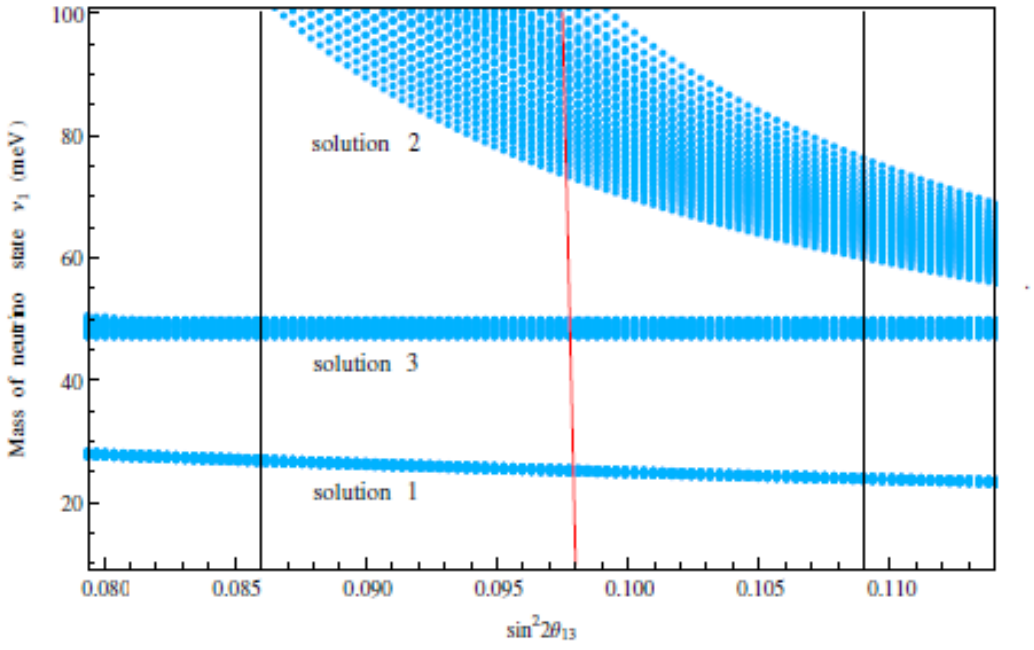

The predicted value of m1 (the mass of the neutrino eigenstate _1) vs the measured value of sin2 2_13. The _nite thickness of the bands is due to the errors in the measurement of the neutrino mass-squared di_erences. The red and the black lines indicate the best _t value and the errors on sin2 2_13 respectively.

Evidence for Direct CP Violation from Dalitz-plot analysis of B± → K±π∓π±

Phys. Rev. D 78 (2008) 012004. DOI: http://dx.doi.org/10.1103/PhysRevD.78.012004

BABAR Collaboration: incl. T. Gershon, P.F. Harrison

We report a Dalitz-plot analysis of the charmless hadronic decays of charged B mesons to the final state $K\pm\pi\mp\pi\pm$. Using a sample of $(383.2\pm4.2)\times106$ $B\overline{B}$ pairs collected by the *BABAR* detector, we measure CP-averaged branching fractions and direct CP asymmetries for intermediate resonant and nonresonant contributions. We find evidence for direct CP violation in the decay $B\pm\rightarrow\rho0(770)K\pm$, with a CP-violation parameter $ACP=(+44\pm10\pm4+5-13)\%$.

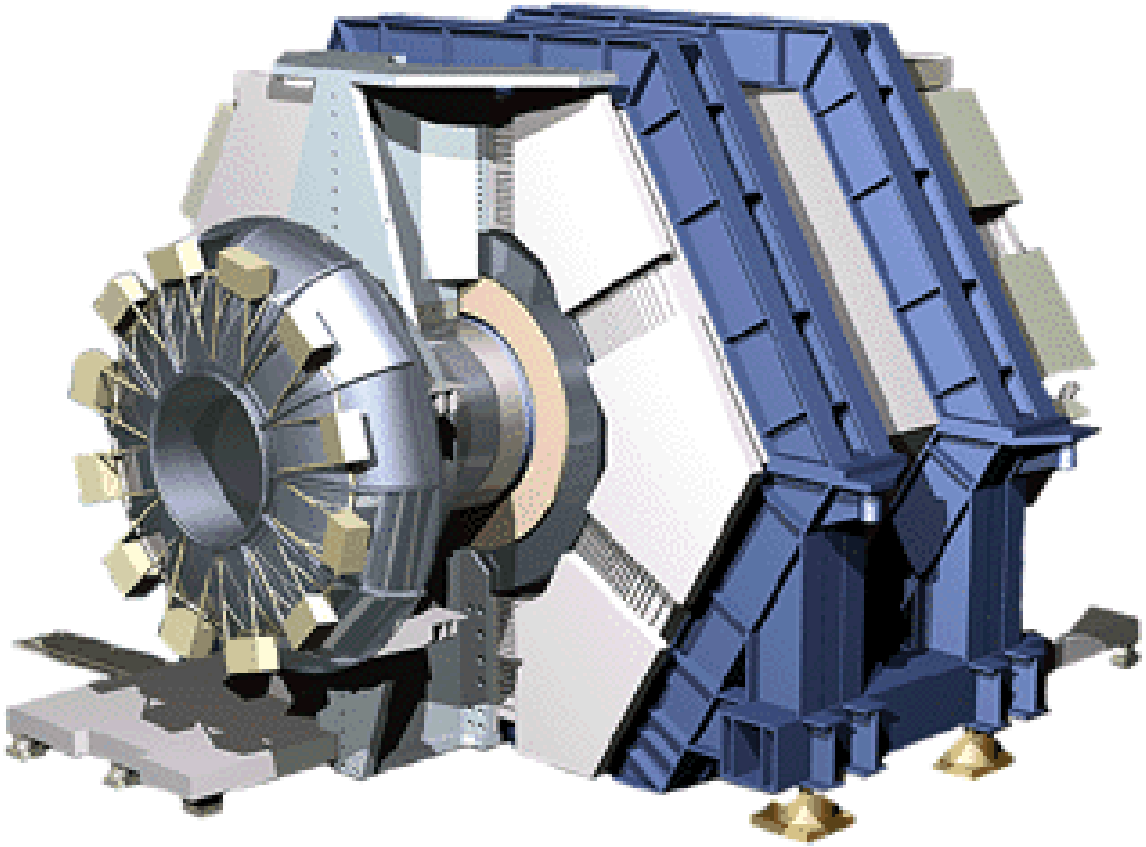

Time-dependent Amplitude Analysis of $B^0 \to K_S \pi^+ \pi^-$

Phys. Rev. D 80, (2009) 112001 DOI: http://dx.doi.org/10.1103/PhysRevD.80.112001

BABAR Collaboration incl. T. Gershon, P.F. Harrison

We perform a time-dependent amplitude analysis of $B0 \to K0S\pi+\pi-$ decays to extract the CP violation parameters of $f0(980)K0S$ and $\rho0(770)K0S$ and the direct CP asymmetry of $K*+(892)\pi-$. The results are obtained from a data sample of $(383\pm3)\times106$ $B\overline{B}$ decays, collected with the *BABAR* detector at the PEP-II asymmetric–energy B factory at SLAC. We find two solutions, with an equivalent goodness-of-fit. Including systematic and Dalitz plot model uncertainties, the combined confidence interval for values of the CP parameter βeff in $B0$ decays to $f0(980)K0S$ is $18°<\beta\text{eff}<76°$ at 95% confidence level (C.L). CP conservation in $B0$ decays to $f0(980)K0S$ is excluded at 3.5 standard deviations including systematic uncertainties. For $B0$ decays to $\rho0(770)K0S$, the combined confidence interval is $-9°<\beta\text{eff}<57°$ at 95% C.L. In decays to $K*+(892)\pi-$ we measure the direct CP asymmetry to be $ACP=-0.20\pm0.10\pm0.01\pm0.02$. The measured phase difference (including $B0\overline{B}0$ mixing) between decay amplitudes of $B0 \to K*+(892)\pi-$ and $\overline{B}0 \to K*-(892)\pi+$, excludes the interval $-137°<\Delta\Phi(K*+(892)\pi-)<-5°$ at 95% C.L.

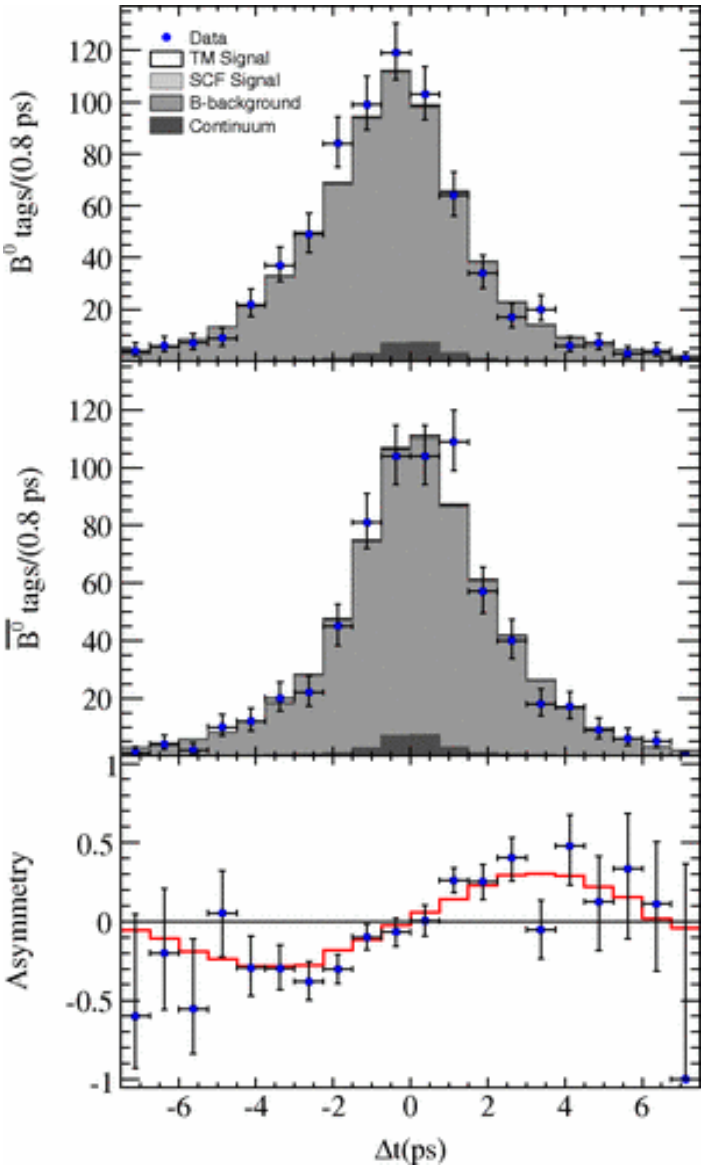

Distributions of Δt when the B_{tag}^{0} is a B^0 (top), $\bar{B}^0$ (middle), and the derived Δt asymmetry (bottom) for events in the $J/\psi K_S^0$ region. The solid line is the total PDF and the points with error bars represent data.

Dalitz Plot Analysis of B+- --> pi+- pi+- pi-+ Decays

Phys. Rev. D 79 (2009) 072006 DOI: http://dx.doi.org/10.1103/PhysRevD.79.072006

BABAR Collaboration incl. T. Gershon, P.F. Harrison

We present a Dalitz plot analysis of charmless $B\pm$ decays to the final state $\pi\pm\pi\pm\pi\mp$ using a sample of (465±5)×106 $B\bar{B}$ pairs collected by the *BABAR* experiment at $s\sqrt{}$=10.58 GeV. We measure the branching fractions B($B\pm\to\pi\pm\pi\pm\pi\mp$)=(15.2±0.6±1.2±0.4)×10−6, B($B\pm\to\rho0(770)\pi\pm$)=(8.1±0.7±1.2+0.4−1.1)×10−6, B($B\pm\to f2(1270)\pi\pm$)=(1.57±0.42±0.16+0.53−0.19)×10−6, and B($B\pm\to\pi\pm\pi\pm\pi\mp$ nonresonant)=(5.3±0.7±0.6+1.1−0.5)×10−6, where the uncertainties are statistical, systematic, and model-dependent, respectively. Measurements of branching fractions for the modes $B\pm\to\rho0(1450)\pi\pm$ and $B\pm\to f0(1370)\pi\pm$ are also presented. We observe no significant direct *CP* asymmetries for the above modes, and there is no evidence for the decays $B\pm\to f0(980)\pi\pm$, $B\pm\to\chi c0\pi\pm$, or $B\pm\to\chi c2\pi\pm$.

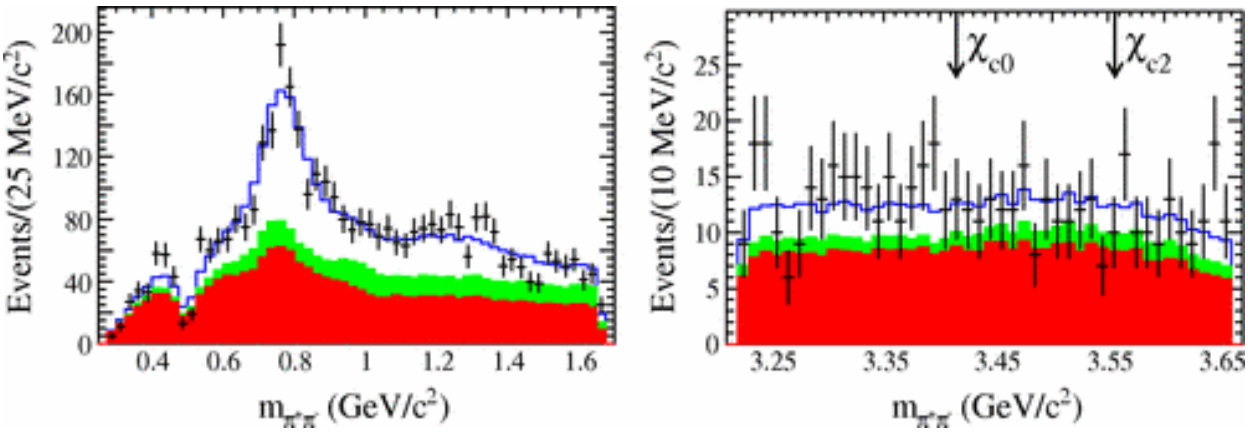

Dipion invariant mass projections: (left) in the $\rho^0(770)$ region; and (right) in the regions of χ_{c0} and χ_{c2}. The data are the points with statistical error bars, the dark-shaded (red) histogram is the $q\bar{q}$ component, the light-shaded (green) histogram is the $B\bar{B}$ background contribution, while the upper (blue) histogram shows the total fit result. The dip near 0.5 GeV/c^2 in the left plot is due to the rejection of events containing K_S^0 candidates.

Differential branching fraction and angular analysis of the decay $B^0 \to K^{*0}\mu^+\mu^-$

Phys. Rev. Lett. 108, 181806 (2012) DOI: http://dx.doi.org/10.1103/PhysRevLett.108.181806

The LHCb collaboration, incl T. Blake, T. Gershon, P.F. Harrison

The angular distributions and the partial branching fraction of the decay $B0 \to K^*0\mu+\mu-$ are studied by using an integrated luminosity of $0.37\ \mathrm{fb}{-1}$ of data collected with the LHCb detector. The forward-backward asymmetry of the muons, $A\mathrm{FB}$, the fraction of longitudinal polarization, $F\mathrm{L}$, and the partial branching fraction $d\mathrm{B}/dq2$ are determined as a function of the dimuon invariant mass. The measurements are in good agreement with the standard model predictions and are the most precise to date. In the dimuon invariant mass squared range $1.00–6.00\ \mathrm{GeV}2/c4$, the results are $A\mathrm{FB}=-0.06+0.13-0.14\pm0.04$, $F\mathrm{L}=0.55\pm0.10\pm0.03$, and $d\mathrm{B}/dq2=(0.42\pm0.06\pm0.03)\times10-7\ c4/\mathrm{GeV}2$. In each case, the first error is statistical and the second systematic.

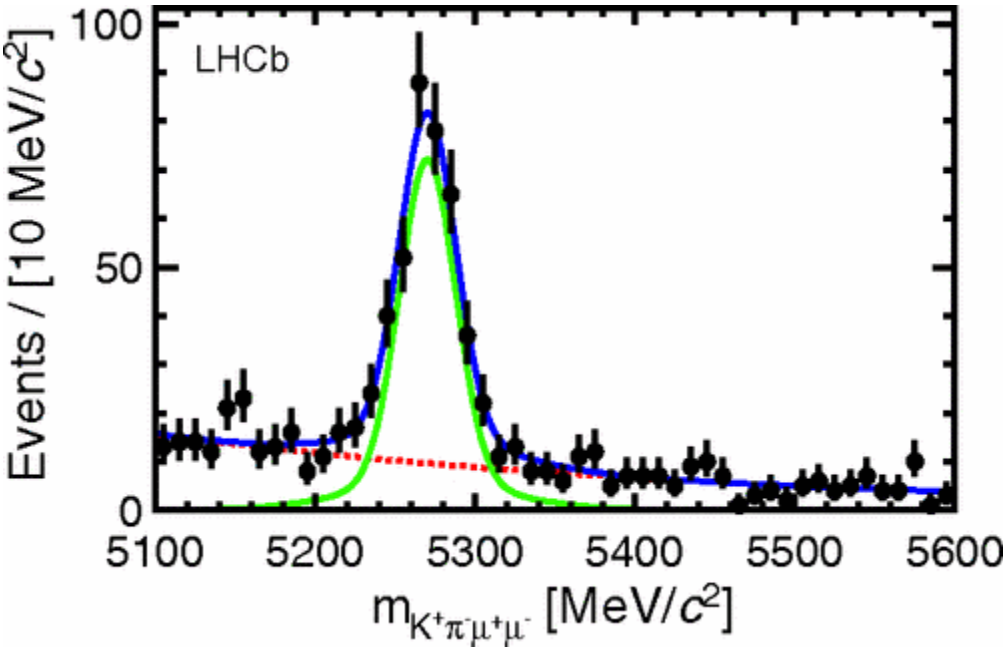

$K^+\pi^-\mu^+\mu^-$ invariant mass distribution after the application of the full selection as data points with the fit overlaid. The signal component is the green (light) line, the background the red (dashed) line, and the full distribution the blue (dark) line.

Evidence for CP violation in time-integrated D0→h−h+ decay rates

Phys. Rev. Lett. 108 (2012) 111602 DOI: http://dx.doi.org/10.1103/PhysRevLett.108.111602

LHCb Collaboration, incl T. Gershon, P.F. Harrison

A search for time-integrated CP violation in $D0\to h-h+$ ($h=K,\pi$) decays is presented using $0.62\ \mathrm{fb}-1$ of data collected by LHCb in 2011. The flavor of the charm meson is determined by the charge of the slow pion in the $D*+\to D0\pi+$ and $D*-\to D\overline{\ }0\pi-$ decay chains. The difference in CP asymmetry between $D0\to K-K+$ and $D0\to\pi-\pi+$, $\Delta ACP\equiv ACP(K-K+)-ACP(\pi-\pi+)$, is measured to be $[-0.82\pm0.21(\mathrm{stat})\pm0.11(\mathrm{syst})]\%$. This differs from the hypothesis of CP conservation by 3.5 standard deviations.

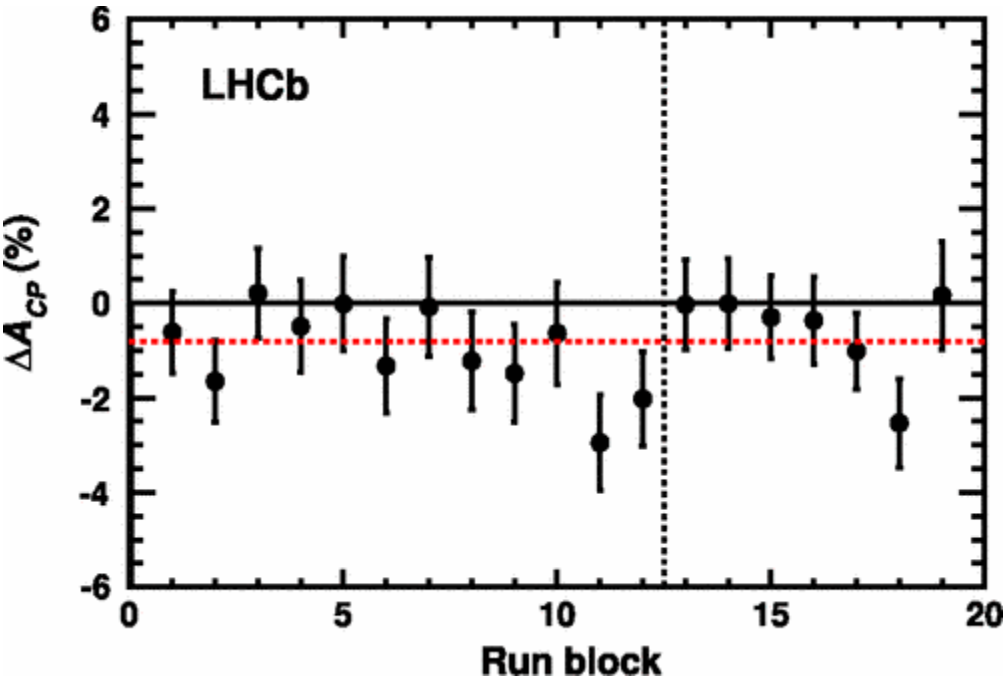

Time dependence of the measurement. The data are divided into 19 disjoint, contiguous, time-ordered blocks and the value of ΔA_{CP} measured in each block. The horizontal red dashed line shows the result for the combined sample.

Search for the lepton number violating decays $B^+ \to \pi^- \mu^+ \mu^+$ and $B^+ \to K^- \mu^+ \mu^+$

Phys. Rev. Lett. 108 (2012) 101601 DOI: http://dx.doi.org/10.1103/PhysRevLett.108.101601

The LHCb collaboration incl T. Blake, T. Gershon, P.F. Harrison

A search is performed for the lepton number violating decay $B^+ \to h^- \mu^+ \mu^+$, where h^- represents a K^- or a π^-, using an integrated luminosity of $36\ \mathrm{pb}^{-1}$ of data collected with the LHCb detector. The decay is forbidden in the standard model but allowed in models with a Majorana neutrino. No signal is observed in either channel and limits of $\mathrm{B}(B^+ \to K^- \mu^+ \mu^+) < 5.4 \times 10^{-8}$ and $\mathrm{B}(B^+ \to \pi^- \mu^+ \mu^+) < 5.8 \times 10^{-8}$ are set at the 95% confidence level. These improve the previous best limits by factors of 40 and 30, respectively.

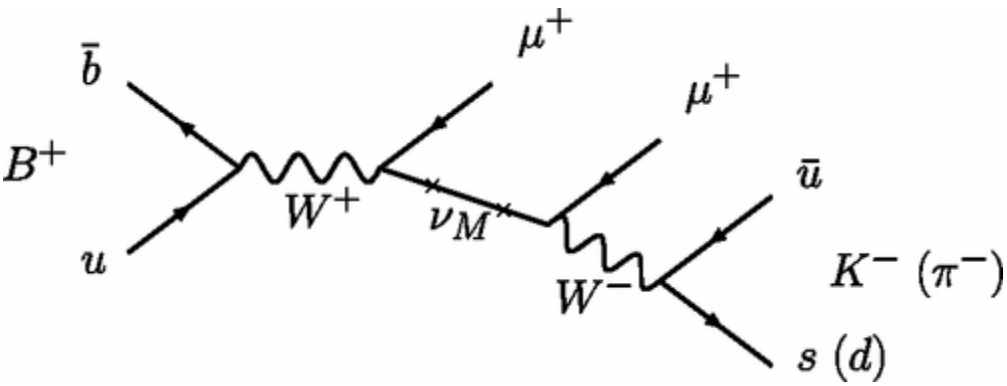

s-channel diagram for $B^+ \to K^- \mu^+ \mu^+$ ($B^+ \to \pi^- \mu^+ \mu^+$) where the decay is mediated by an on-shell Majorana neutrino

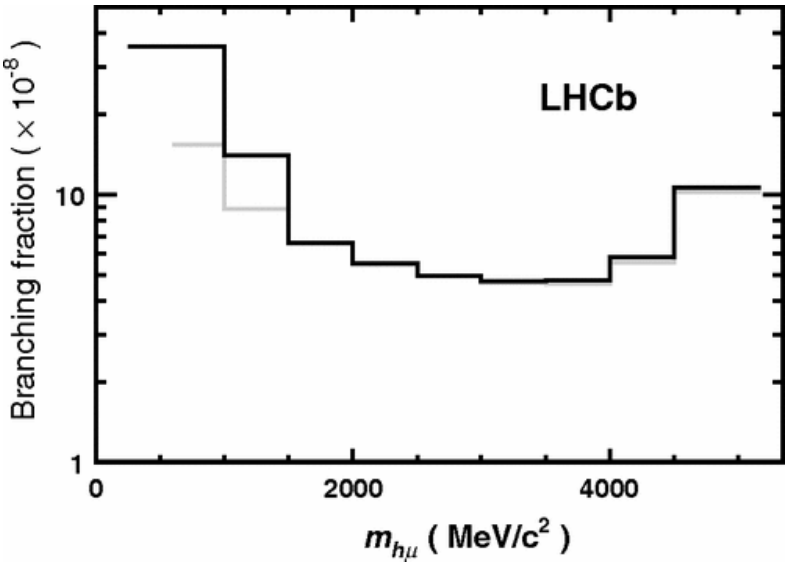

The 95% C.L. branching fraction limits for $B^+ \to K^- \mu^+ \mu^+$ (light-colored line) and $B^+ \to \pi^- \mu^+ \mu^+$ (dark-colored line) as a function of the Majorana neutrino mass $m_\nu = m_{h\mu}$.

Performance of the LHCb RICH detector at the LHC

Eur. Phys. J. C 73, 2431 (2013)

The LHCb collaboration incl T. Blake, T. Gershon, P.F. Harrison

The LHCb experiment has been taking data at the Large Hadron Collider (LHC) at CERN since the end of 2009. One of its key detector components is the Ring-Imaging Cherenkov (RICH) system. This provides charged particle identification over a wide momentum range, from 2–100 GeV/*c*. The operation and control, software, and online monitoring of the RICH system are described. The particle identification performance is presented, as measured using data from the LHC. Excellent separation of hadronic particle types (π, K, p) is achieved.

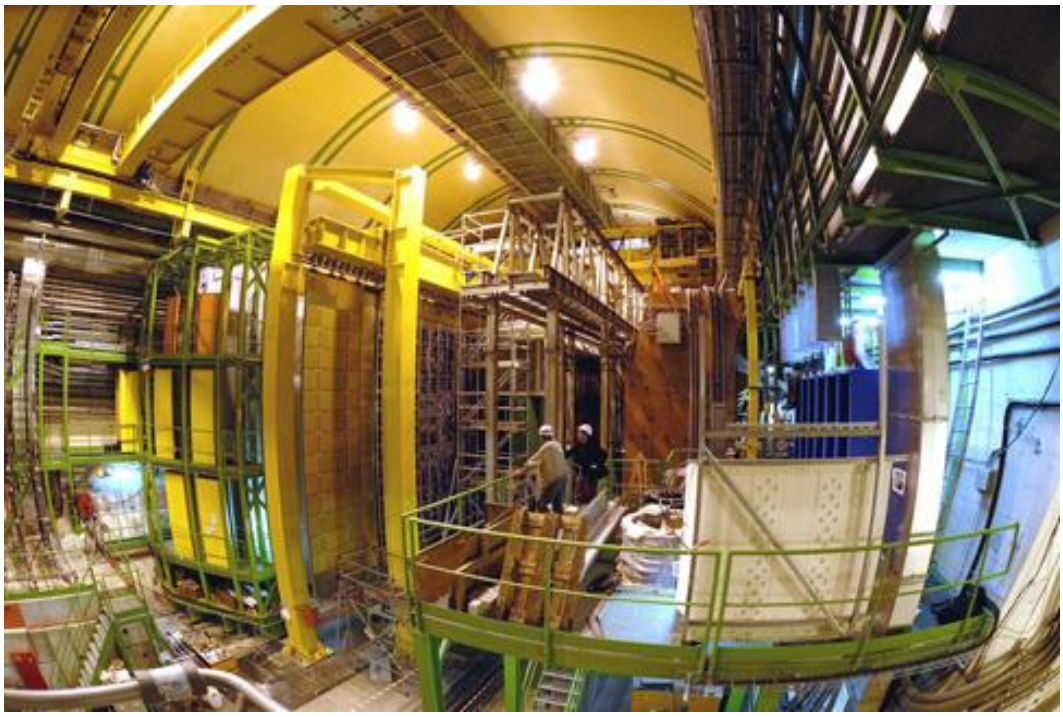

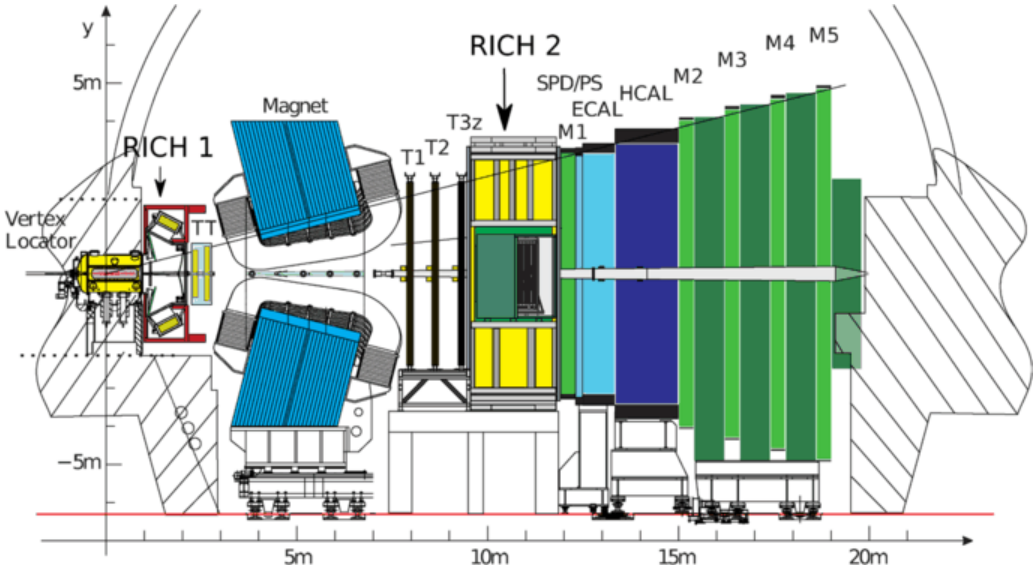

Side view of the LHCb spectrometer, with the two RICH detectors indicated

First Evidence for the Decay $B^0_s \to \mu^+\mu^-$

Phys. Rev. Lett. 110 (2013) 021801 DOI: http://dx.doi.org/10.1103/PhysRevLett.110.021801

LHCb Collaboration, incl T. Gershon, P.F. Harrison

A search for the rare decays $B0s \to \mu+\mu-$ and $B0 \to \mu+\mu-$ is performed with data collected in 2011 and 2012 with the LHCb experiment at the Large Hadron Collider. The data samples comprise $1.1\ \mathrm{fb}{-1}$ of proton-proton collisions at $s\sqrt{=8}\ \mathrm{TeV}$ and $1.0\ \mathrm{fb}{-1}$ at $s\sqrt{=7}\ \mathrm{TeV}$. We observe an excess of $B0s \to \mu+\mu-$ candidates with respect to the background expectation. The probability that the background could produce such an excess or larger is $5.3\times10{-4}$ corresponding to a signal significance of 3.5 standard deviations. A maximum-likelihood fit gives a branching fraction of $\mathrm{B}(B0s \to \mu+\mu-)=(3.2+1.5{-}1.2)\times10{-}9$, where the statistical uncertainty is 95% of the total uncertainty. This result is in agreement with the standard model expectation. The observed number of $B0 \to \mu+\mu-$ candidates is consistent with the background expectation, giving an upper limit of $\mathrm{B}(B0 \to \mu+\mu-)<9.4\times10{-}10$ at 95% confidence level.

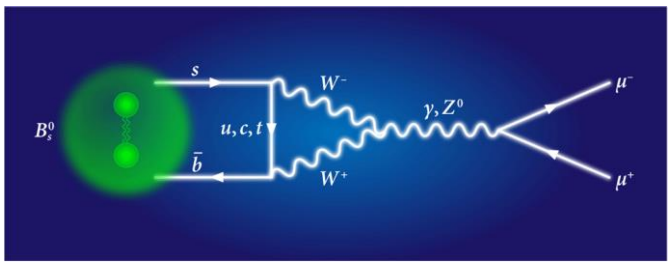

A Feynman diagram represents the decay of a neutral *B*-meson, B_s^0, to a pair of muons, $\mu^+\mu^-$. The green sphere on the left indicates the meson, which is a bound state of a strange quark and an antibottom quark. These radiate two *W* bosons and exchange a top quark in the process. The *W* bosons fuse to a *Z* boson, which then produces the two muons in the final state.

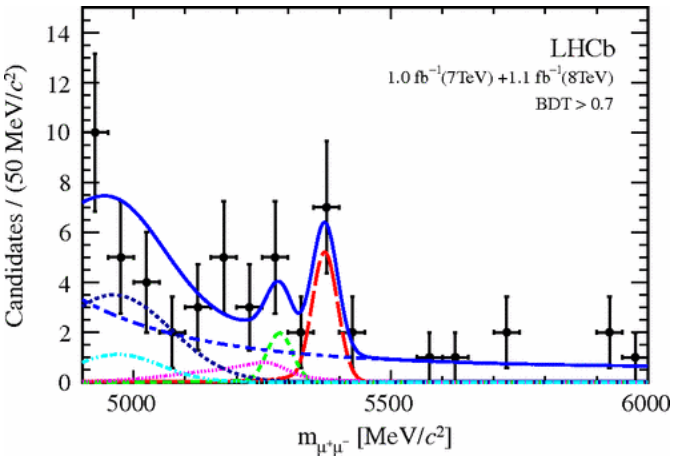

Invariant mass distribution of the selected $B_s^0 \to \mu^+\mu^-$ candidates (black dots) with BDT>0.7 in the combined 2011 and 2012 data sets. The result of the fit is overlaid (blue solid line) and the different components detailed: $B_s^0 \to \mu^+\mu^-$ (red long dashed curve), $B^0 \to \mu^+\mu^-$ (green medium dashed curve), $B_{(s)}^0 \to h^+h'^-$ (pink dotted curve), $B^0 \to \pi^-\mu^+\nu_\mu$ (black short dashed curve), and $B^{0(+)} \to \pi^{0(+)}\mu^+\mu^-$ (light blue dash-dotted curve), and the combinatorial background (blue medium dashed).

On the Measurement of the Unitarity Triangle Angle γ from $B^0 \to DK^{*0}$ Decays.

Phys. Rev. D 79 (2009) 051301 DOI: http://dx.doi.org/10.1103/PhysRevD.79.051301

Tim Gershon

The decay $B0 \to DK^{*}0$ is well known to provide excellent potential for a precise measurement of the unitarity triangle angle γ in future experiments. It is noted that the sensitivity can be significantly enhanced by studying the amplitudes relative to those of the flavor-specific decay $B0 \to D^{*-}2K+$, which can be achieved by analyzing the $B0 \to D\pi-K+$ Dalitz plot.

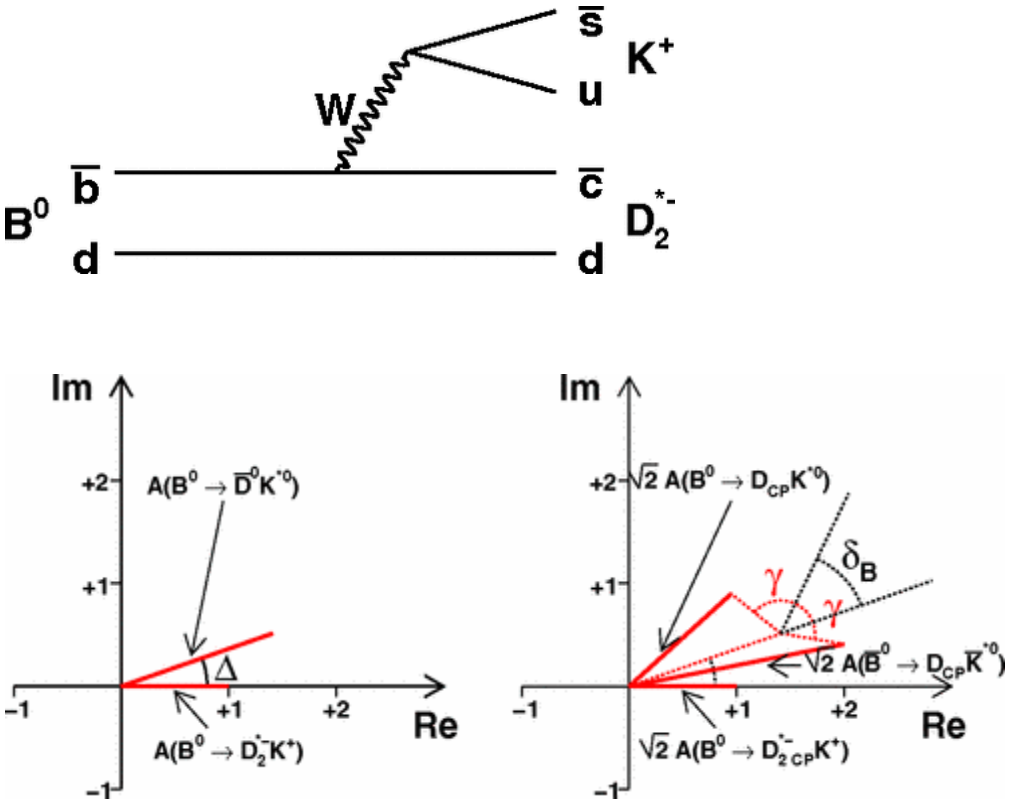

Argand diagrams illustrating the measurements of relative amplitudes and phases from analysis of the Dalitz plots of (left) $D^{0}\pi^{-}K^{+}$ and (right) $D_{CP}\pi^{-}K^{+}$. In these illustrative examples the following values are used: $|A(B^0 \to D^{0}K^{*0})/A(B^0 \to D_2^{*-}K^{+})|=1.5$, $\Delta=\arg(A(B^0 \to D^{0}K^{*0})/A(B^0 \to D_2^{*-}K^{+}))=20°$, $\gamma=75°$, $\delta_B=45.0°$ and $r_B=0.4$. These are in line with expectation and current measurements, though Δ and δ_B are unconstrained at present.

First observations of $\bar{B}_S^0 \to D^+D^-$, $D_S\, D^-$ and $D^0\bar{D}^0$ decays

Physical Review D , 87, (2013)

LHCb collaboration inc T. Gershon

First observations and measurements of the branching fractions of the B¯ºs →D+D-, B¯ºs →Ds+D- and B¯ºs→DºD¯º decays are presented using 1.0 fb-1 of data collected by the LHCb experiment. These branching fractions are normalized to those of B¯ºs →D+D, Bº→D-Ds+ and B¯→DºD¯s, respectively. An excess of events consistent with the decay B¯º →DºD¯º is also seen, and its branching fraction is measured relative to that of B¯→DºD¯s. Improved measurements of the branching fractions B(B¯ºs→Ds+Ds-) and B(B¯→DºDs-) are reported, each relative to B(Bº→D-Ds+). The ratios of branching fractions are B(B¯ºs →D+D-) B(B¯ºs→DºD¯º)=1.08±0.20±0.10, B(B¯ºs →D+D-) B(Bº→D-Ds+)=0.050±0.008±0.004, B(B¯ºs→DºD¯º)/B(B¯→DºD¯s)=0.019±0.003±0.003, B(B¯ºs→DºD¯º)/B(B¯→DºD¯s)<0.0024 at 90% CL, B(B¯ºs →D+D-) B(Bº→D-Ds+)=0.56±0.03±0.04, B(B¯→DºD¯s)/B(Bº→D-Ds+)=1.22±0.02±0.07, where the uncertainties are statistical and systematic, respectively.

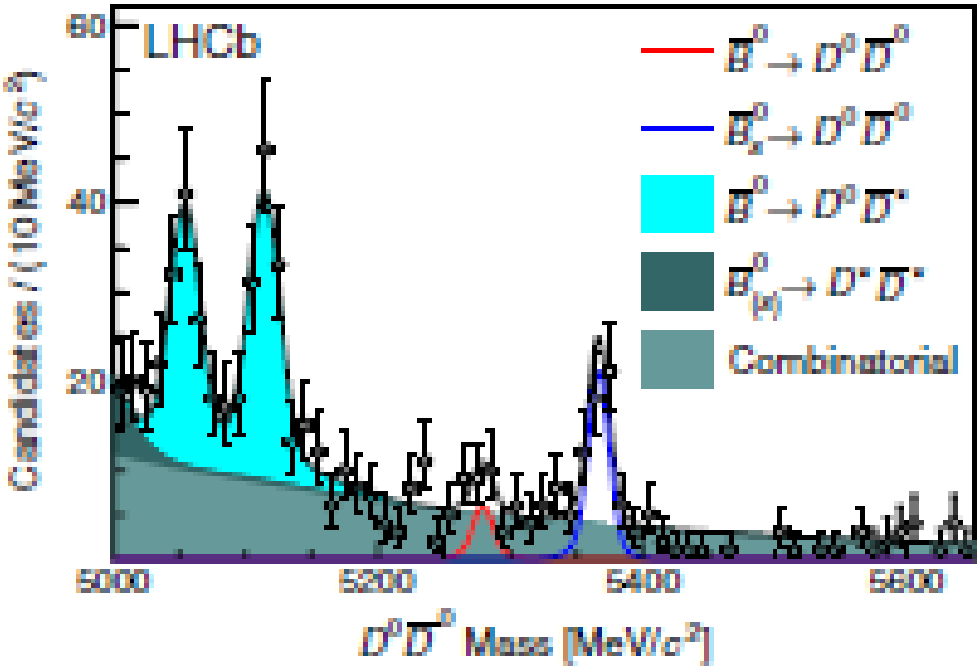

Implications of LHCb measurements and future prospects

European Physical Journal C, April 2013, Volume 73, pp2373

LHCb collaboration inc T. Gershon

During 2011 the LHCb experiment at CERN collected 1.0 fb−1 of √s=7~TeV pp collisions. Due to the large heavy quark production cross-sections, these data provide unprecedented samples of heavy flavoured hadrons. The first results from LHCb have made a significant impact on the flavour physics landscape and have definitively proved the concept of a dedicated experiment in the forward region at a hadron collider. This document discusses the implications of these first measurements on classes of extensions to the Standard Model, bearing in mind the interplay with the results of searches for on-shell production of new particles at ATLAS and CMS. The physics potential of an upgrade to the LHCb detector, which would allow an order of magnitude more data to be collected, is emphasised.

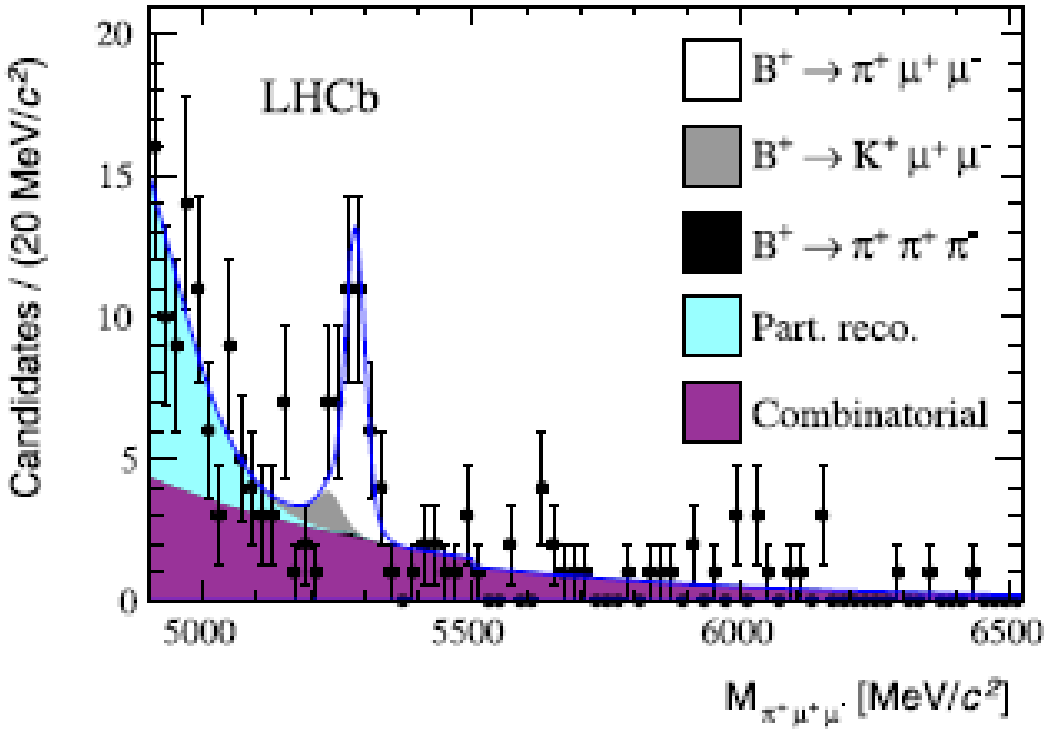

Observation of a centrality-dependent Dijet Asymmetry in Lead-Lead Collisions at sqrt(S(NN))=2.76TeV with the ATLAS detector at the LHC

Phys. Rev. Lett. 105 (2010) 252303 DOI: http://dx.doi.org/10.1103/PhysRevLett.105.252303

The ATLAS collaboration

By using the ATLAS detector, observations have been made of a centrality-dependent dijet asymmetry in the collisions of lead ions at the Large Hadron Collider. In a sample of lead-lead events with a per-nucleon center of mass energy of 2.76 TeV, selected with a minimum bias trigger, jets are reconstructed in fine-grained, longitudinally segmented electromagnetic and hadronic calorimeters. The transverse energies of dijets in opposite hemispheres are observed to become systematically more unbalanced with increasing event centrality leading to a large number of events which contain highly asymmetric dijets. This is the first observation of an enhancement of events with such large dijet asymmetries, not observed in proton-proton collisions, which may point to an interpretation in terms of strong jet energy loss in a hot, dense medium.

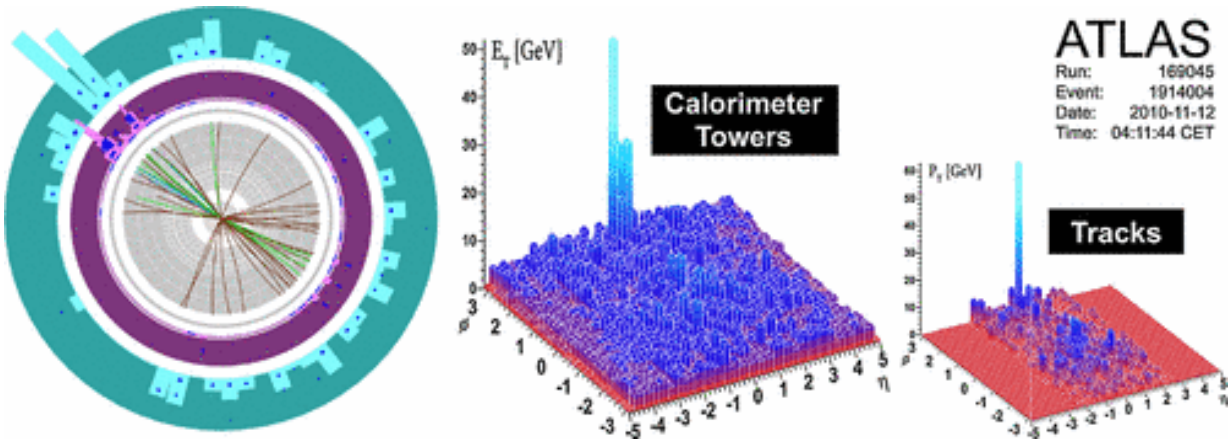

Event display of a highly asymmetric dijet event, with one jet with E_T>100 GeV and no evident recoiling jet and with high-energy calorimeter cell deposits distributed over a wide azimuthal region. By selecting tracks with p_T>2.6 GeV and applying cell thresholds in the calorimeters (E_T>700 MeV in the electromagnetic calorimeter, and E>1 GeV in the hadronic calorimeter), the recoil can be seen dispersed widely over the azimuth

Measurement of the Z -> tau tau cross section with the ATLAS detector

Phys. Rev. D, 84 (2011) 112006 DOI: http://dx.doi.org/10.1103/PhysRevD.84.112006

The ATLAS collaboration

The $Z \to \tau\tau$ cross section is measured with the ATLAS experiment at the LHC in four different final states determined by the decay modes of the τ leptons: muon-hadron, electron-hadron, electron-muon, and muon-muon. The analysis is based on a data sample corresponding to an integrated luminosity of $36\ \mathrm{pb}^{-1}$, at a proton-proton center-of-mass energy of $\sqrt{s}=7\ \mathrm{TeV}$. Cross sections are measured separately for each final state in fiducial regions of high detector acceptance, as well as in the full phase space, over the mass region 66–116 GeV. The individual cross sections are combined and the product of the total Z production cross section and $Z \to \tau\tau$ branching fraction is measured to be $0.97 \pm 0.07(\mathrm{stat}) \pm 0.06(\mathrm{syst}) \pm 0.03(\mathrm{lumi})\ \mathrm{nb}$, in agreement with next-to-next-to-leading order calculations.

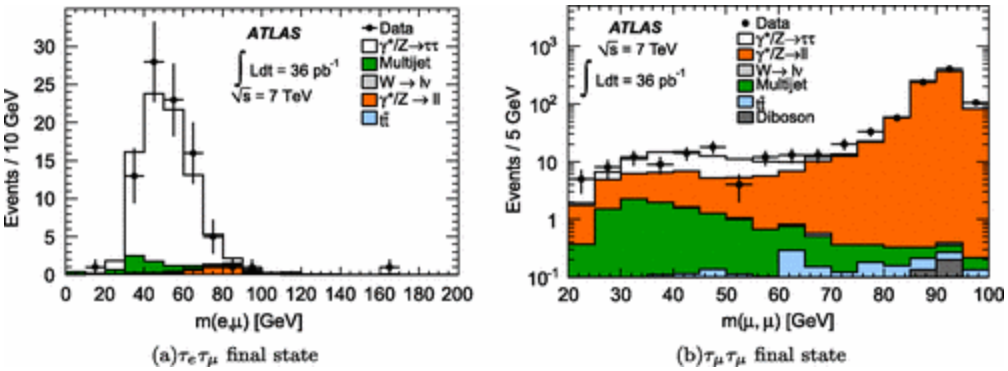

The distributions of the visible mass for the (a) $\tau_e\tau_\mu$ and (b) $\tau_\mu\tau_\mu$ final states,

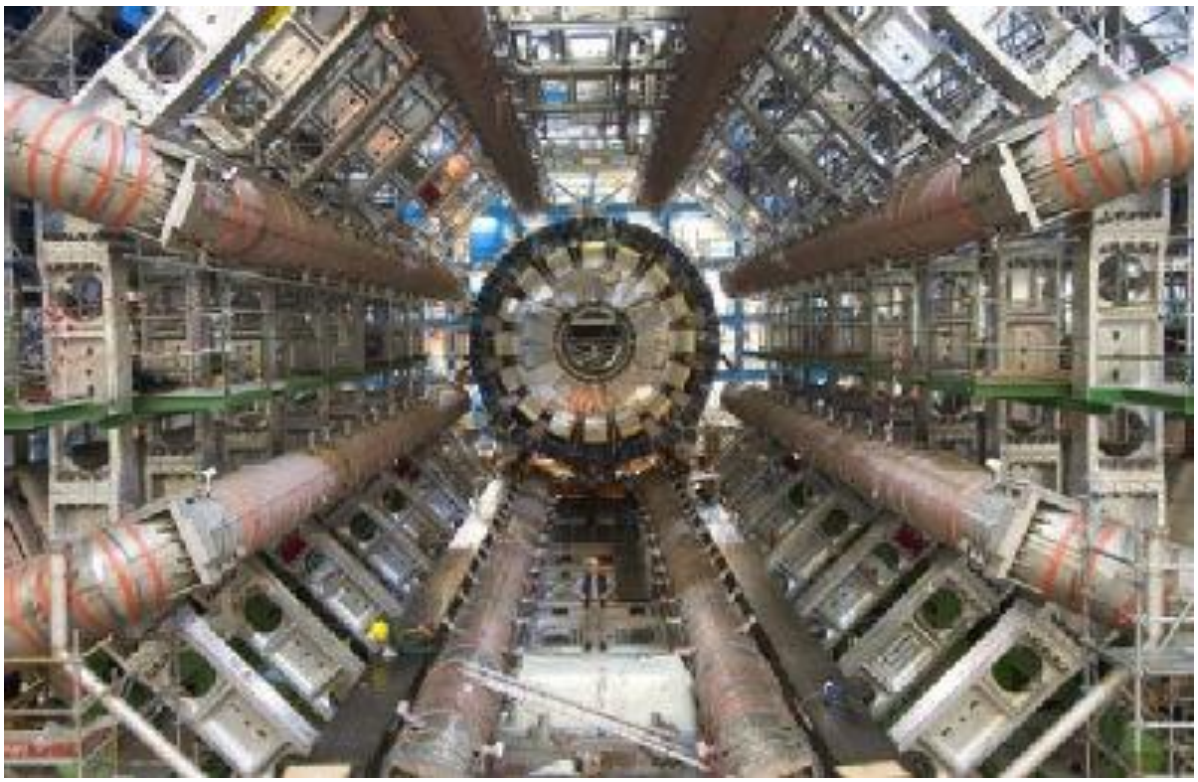

Combined search for the Standard Model Higgs boson using up to 4.9 fb^{-1} of pp collision data at $\sqrt{s}$=7 TeV with the ATLAS detector at the LHC

Physics Letters B 710, 49 (2012) doi:10.1016/j.physletb.2012.02.044

The ATLAS collaboration

A combined search for the Standard Model Higgs boson with the ATLAS experiment at the LHC using datasets corresponding to integrated luminosities from 1.04 fb^{-1} to 4.9 fb^{-1} of pp collisions collected at $\sqrt{s} = 7$ TeV s=7 TeV is presented. The Higgs boson mass ranges 112.9–115.5 GeV, 131–238 GeV and 251–466 GeV are excluded at the 95% confidence level (CL), while the range 124–519 GeV is expected to be excluded in the absence of a signal. An excess of events is observed around m_H~126 GeVmH~126 GeV with a local significance of 3.5 standard deviations (σ). The local significances of H→γγH→γγ, $H \to ZZ^{(*)} \to \ell^+\ell^-\ell'^+\ell'^-$ H→ZZ(⍰)→ℓ+ℓ−ℓ′+ℓ′− and $H \to WW^{(*)} \to \ell^+\nu\ell'^-\bar{\nu}$ H→WW(⍰)→ℓ+νℓ′−ν¯, the three most sensitive channels in this mass range, are 2.8σ , 2.1σ and 1.4σ , respectively. The global probability for the background to produce such a fluctuation anywhere in the explored Higgs boson mass range 110–600 GeV is estimated to be ~1.4%~1.4% or, equivalently, 2.2σ.

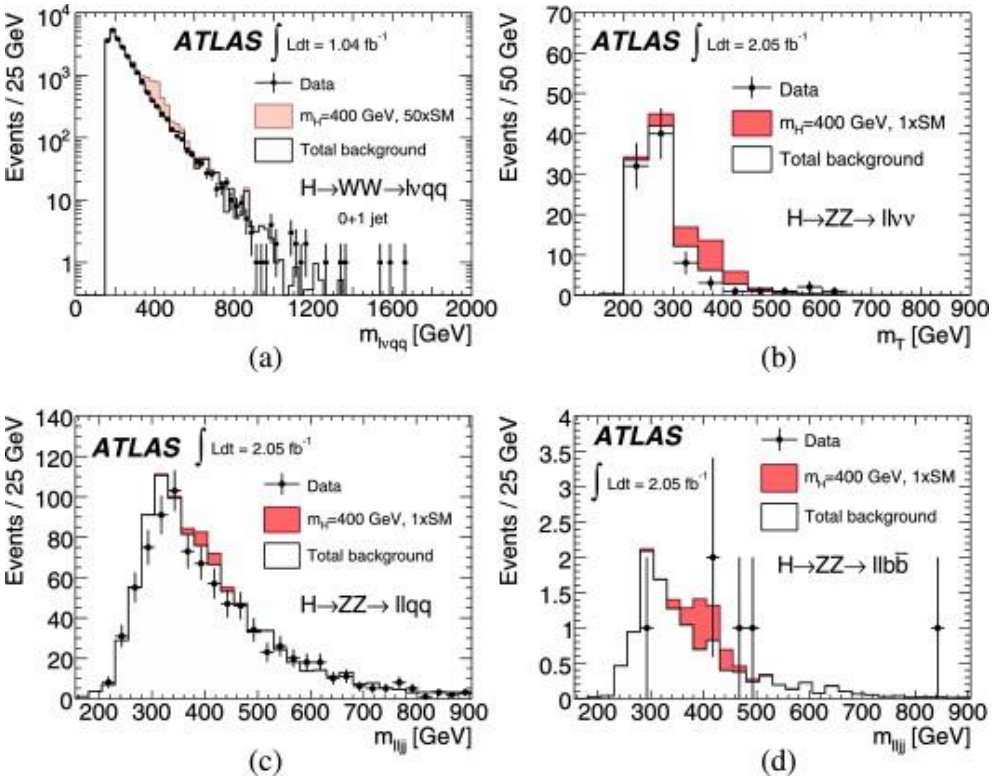

Distributions of the reconstructed invariant or transverse mass, in analyses relevant for the search of the Higgs boson at high mass, for selected candidate events, the total background and the signal (m_H=400 GeVmH=400 GeV) expected for the given value of m_HmH in the $H \to WW \to \ell\nu q\bar{q}'$ H→WW→ℓνqq¯′ channel (a), the $H \to ZZ \to \ell^+\ell^-\nu\bar{\nu}$ H→ZZ→ℓ+ℓ−νν¯ channel (b) and the $H \to ZZ \to \ell^+\ell^-q\bar{q}$ H→ZZ→ℓ+ℓ−qq¯ channel for events selected in the b -jet untagged (c) and the tagged (d) categories. The signal distribution is displayed in a lighter red colour in the $H \to WW \to \ell\nu q\bar{q}'$ H→WW→ℓνqq¯′ channel where it has been scaled up by a factor 50.

Search for the Standard Model Higgs boson in the decay channel H -> ZZ(*) -> 4l with 4.8 fb-1 of pp collision data at sqrt[s]=7 TeV with ATLAS

Physics Letters B 710, 383(2012) doi:10.1016/j.physletb.2012.03.005

The ATLAS collaboration

This Letter presents a search for the Standard Model Higgs boson in the decay channel $H \to ZZ^{(*)} \to \ell^+\ell^-\ell'^+\ell'^-$H→ZZ(⍰)→ℓ+ℓ−ℓ′+ℓ′−, where ℓ,ℓ′=eℓ,ℓ′=e or μ , using proton–proton collisions at $\sqrt{s} = 7$ TeV s=7 TeV recorded with the ATLAS detector and corresponding to an integrated luminosity of 4.8 fb^{-1}. The four-lepton invariant mass distribution is compared with Standard Model background expectations to derive upper limits on the cross section of a Standard Model Higgs boson with a mass between 110 GeV and 600 GeV. The mass ranges 134–156 GeV, 182–233 GeV, 256–265 GeV and 268–415 GeV are excluded at the 95% confidence level. The largest upward deviations from the background-only hypothesis are observed for Higgs boson masses of 125 GeV, 244 GeV and 500 GeV with local significances of 2.1, 2.2 and 2.1 standard deviations, respectively. Once the look-elsewhere effect is considered, none of these excesses are significant.

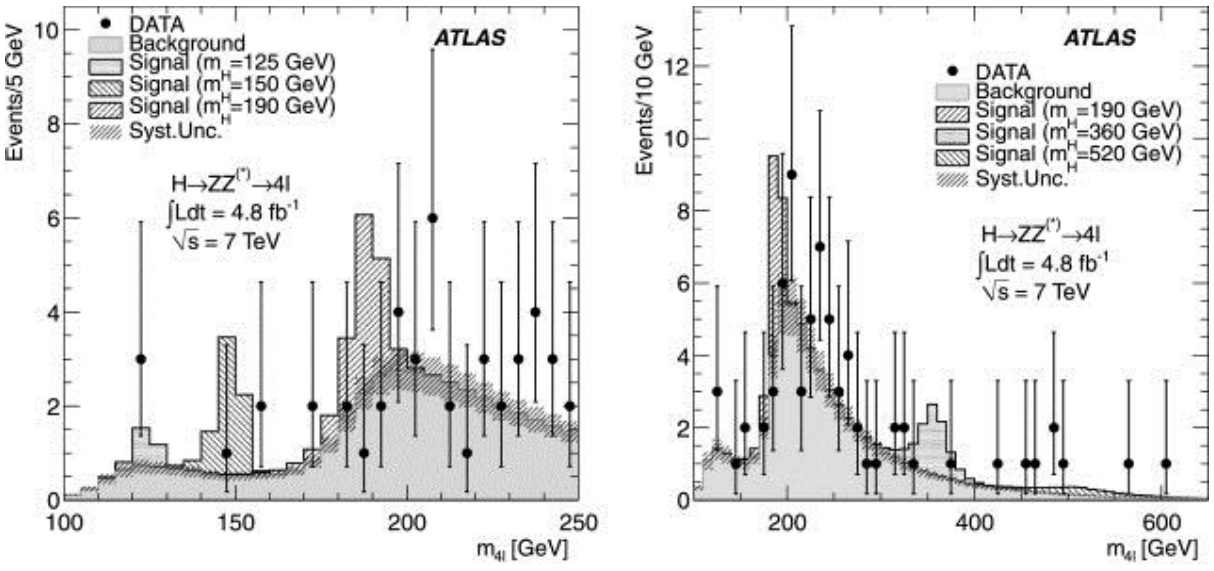

m4ℓm4ℓ distribution of the selected candidates, compared to the background expectation for (a) the 100–250 GeV mass range and (b) the full mass range of the analysis. Error bars represent 68.3% central confidence intervals. The signal expectation for several mHmH hypotheses is also shown. The resolution of the reconstructed Higgs mass is dominated by detector resolution at low mHmH values and by the Higgs boson width at high mHmH.

Search for events with large missing transverse momentum, jets, and at least two tau leptons in 7 TeV proton-proton collision data with the ATLAS detector

Physics Letters B 714, (2012), 180-196 doi:10.1016/j.physletb.2012.06.055

The ATLAS collaboration

A search for events with large missing transverse momentum, jets, and at least two tau leptons has been performed using 2 fb^{-1} of proton–proton collision data at $\sqrt{s} = 7$ TeV s=7 TeV recorded with the ATLAS detector at the Large Hadron Collider. No excess above the Standard Model background expectation is observed and a 95% CL upper limit on the visible cross section for new phenomena is set, where the visible cross section is defined by the product of cross section, branching fraction, detector acceptance and event selection efficiency. A 95% CL lower limit of 32 TeV is set on the gauge-mediated supersymmetry breaking (GMSB) scale Λ independent of tan β. These limits provide the most stringent tests to date in a large part of the considered parameter space.

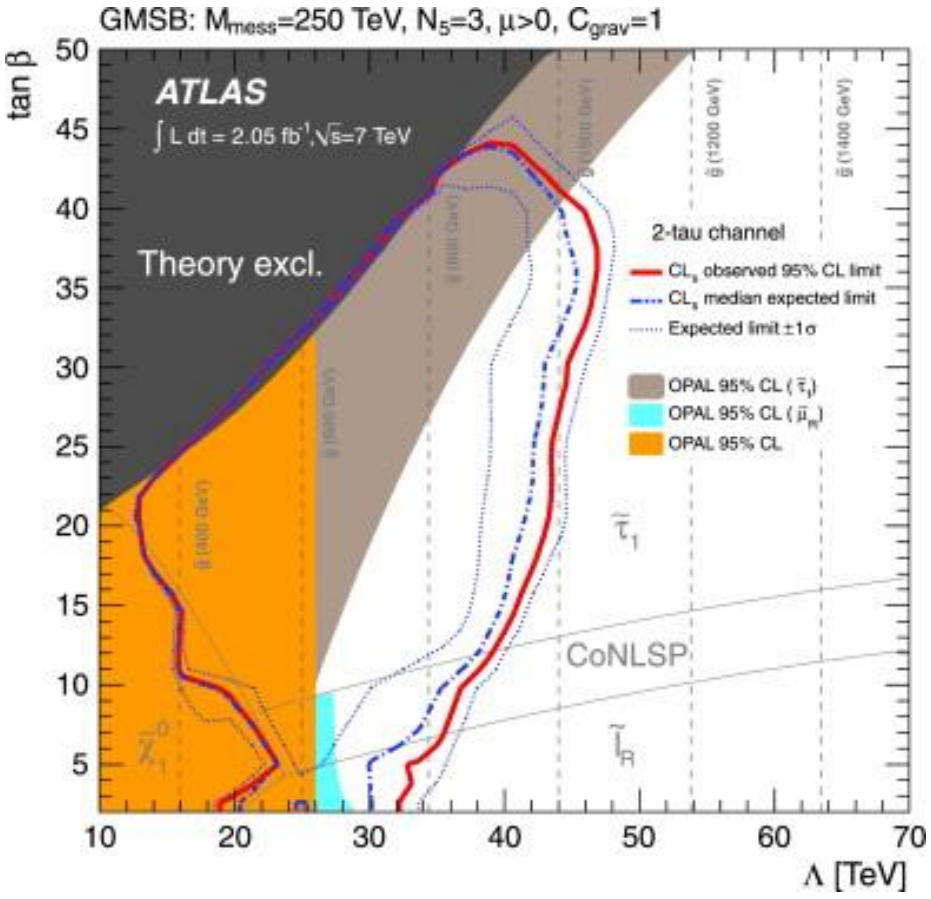

Expected and observed 95% CL limits on the minimal GMSB model parameters Λ and tan β . The dark grey area indicates the region which is theoretically excluded due to unphysical sparticle mass values. The different NLSP regions are indicate. In the CoNLSP region the $\tilde{\tau}_1$τ˜1 and the $\tilde{\ell}_R$ℓ˜R are the NLSP. Additional model parameters are M_{mess}=250 TeVMmess=250 TeV, N_5=3N5=3, μ > 0 and C_{grav}=1Cgrav=1. The previous OPAL [19] limits are also shown.

Search for supersymmetry with jets, missing transverse momentum and at least one hadronically decaying tau lepton in proton-proton collisions at sqrt{s} = 7 TeV with the ATLAS detector

Physics Letters B 714, (2012), 197-214 doi:10.1016/j.physletb.2012.06.061

The ATLAS collaboration

A search for production of supersymmetric particles in final states containing jets, missing transverse momentum, and at least one hadronically decaying τ lepton is presented. The data were recorded by the ATLAS experiment in $\sqrt{s} = 7$ TeV s=7 TeV proton–proton collisions at the Large Hadron Collider. No excess above the Standard Model background expectation was observed in $2.05\ \text{fb}^{-1}$ 2.05fb−1 of data. The results are interpreted in the context of gauge mediated supersymmetry breaking models with $_{\text{Mmess}}$=250 TeVMmess=250 TeV, $_{N5}$=3N5=3, μ>0μ>0, and $_{\text{Cgrav}}$=1Cgrav=1. The production of supersymmetric particles is excluded at 95% C.L. up to a supersymmetry breaking scale Λ=30 TeVΛ=30 TeV, independent of tan β , and up to Λ=43 TeVΛ=43 TeV for large tan β.

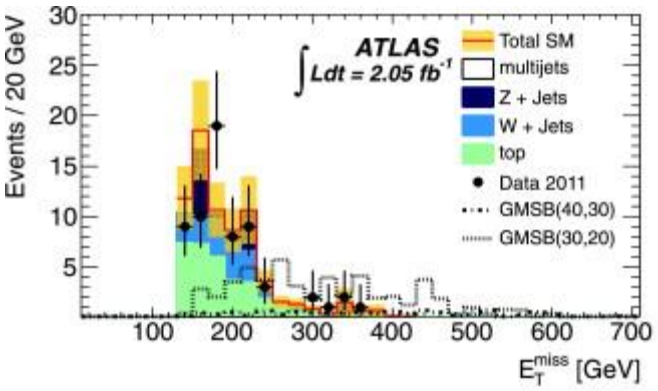

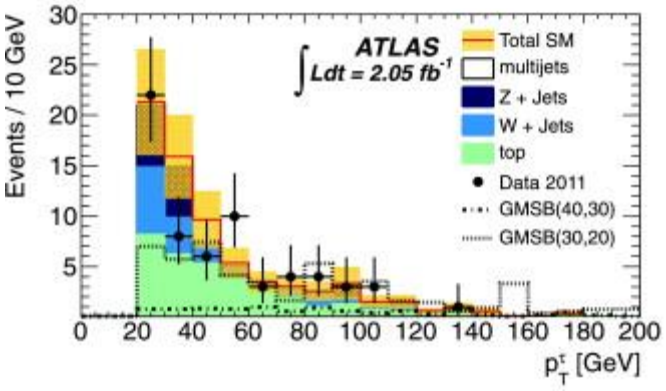

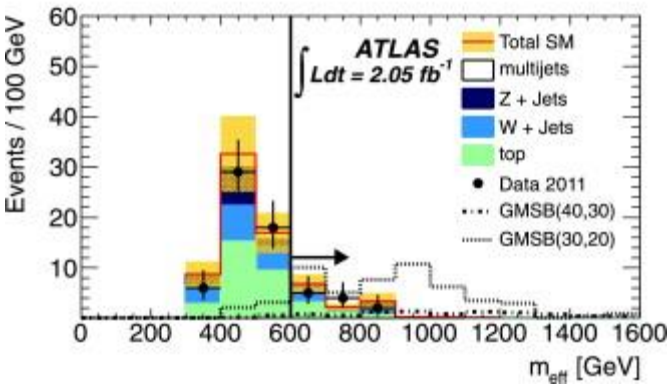

Distributions of $E_{\text{T}}^{\text{miss}}$ ETmiss, p_{T}^{τ} pTτ, and $_{\text{meff}}$meff for data with all selection requirements except for that on $_{\text{meff}}$meff, along with the corresponding estimated backgrounds. Backgrounds are taken from simulation and normalized with control regions in data. The solid (red) line with shaded (yellow) error band corresponds to the total SM prediction, while the points are data. The error bands indicate the size of the total (statistical and systematic) uncertainty. The notation GMSB(40,30) stands for the GMSB model with Λ = 40 TeV and tan β = 30 and analogously for GMSB(30,20)

Observation of a new particle in the search for the Standard Model Higgs boson with the ATLAS detector at the LHC

Physics Letters B 716 (2012) 1-29 10.1016/j.physletb.2012.08.020

The ATLAS collaboration, incl. S. M. Farrington, M. Janus, W.J. Murray

A search for the Standard Model Higgs boson in proton-proton collisions with the ATLAS detector at the LHC is presented. The datasets used correspond to integrated luminosities of approximately 4.8 fb^-1 collected at sqrt(s) = 7 TeV in 2011 and 5.8 fb^-1 at sqrt(s) = 8 TeV in 2012. Individual searches in the channels H->ZZ^(*)->llll, H->gamma gamma and H->WW->e nu mu nu in the 8 TeV data are combined with previously published results of searches for H->ZZ^(*), WW^(*), bbbar and tau^+tau^- in the 7 TeV data and results from improved analyses of the H->ZZ^(*)->llll and H->gamma gamma channels in the 7 TeV data. Clear evidence for the production of a neutral boson with a measured mass of 126.0 +/- 0.4(stat) +/- 0.4(sys) GeV is presented. This observation, which has a significance of 5.9 standard deviations, corresponding to a background fluctuation probability of 1.7x10^-9, is compatible with the production and decay of the Standard Model Higgs boson.

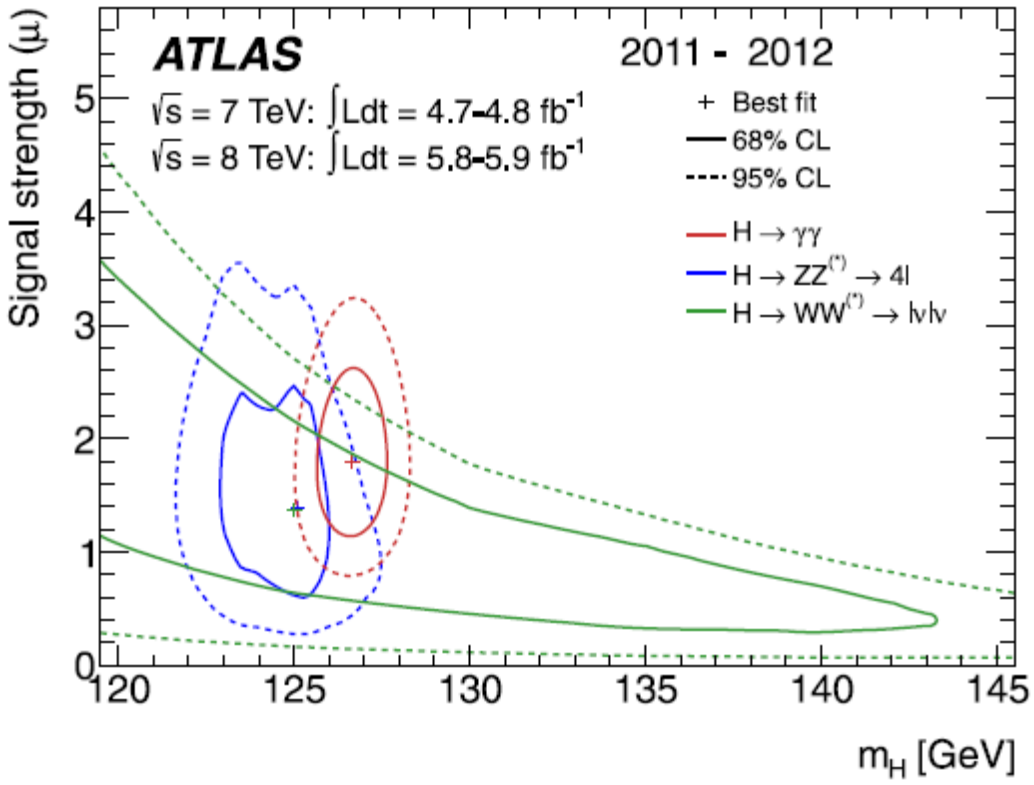

Search for the Standard Model Higgs boson in the H -> tau tau decay mode in sqrt(s) = 7 Tev pp collisions with ATLAS

JHEP 09 (2012) 070 DOI: 10.1007/JHEP09(2012)070

The ATLAS collaboration

A search for the Standard Model Higgs boson decaying into a pair of tau leptons is reported. The analysis is based on a data sample of proton-proton collisions collected by the ATLAS experiment at the LHC and corresponding to an integrated luminosity of 4.7 fb^-1. No significant excess over the expected background is observed in the Higgs boson mass range of 100-150 GeV. The observed (expected) upper limits on the cross section times the branching ratio for H to tau+ tau- are found to be between 2.9 (3.4) and 11.7 (8.2) times the Standard Model prediction for this mass range.

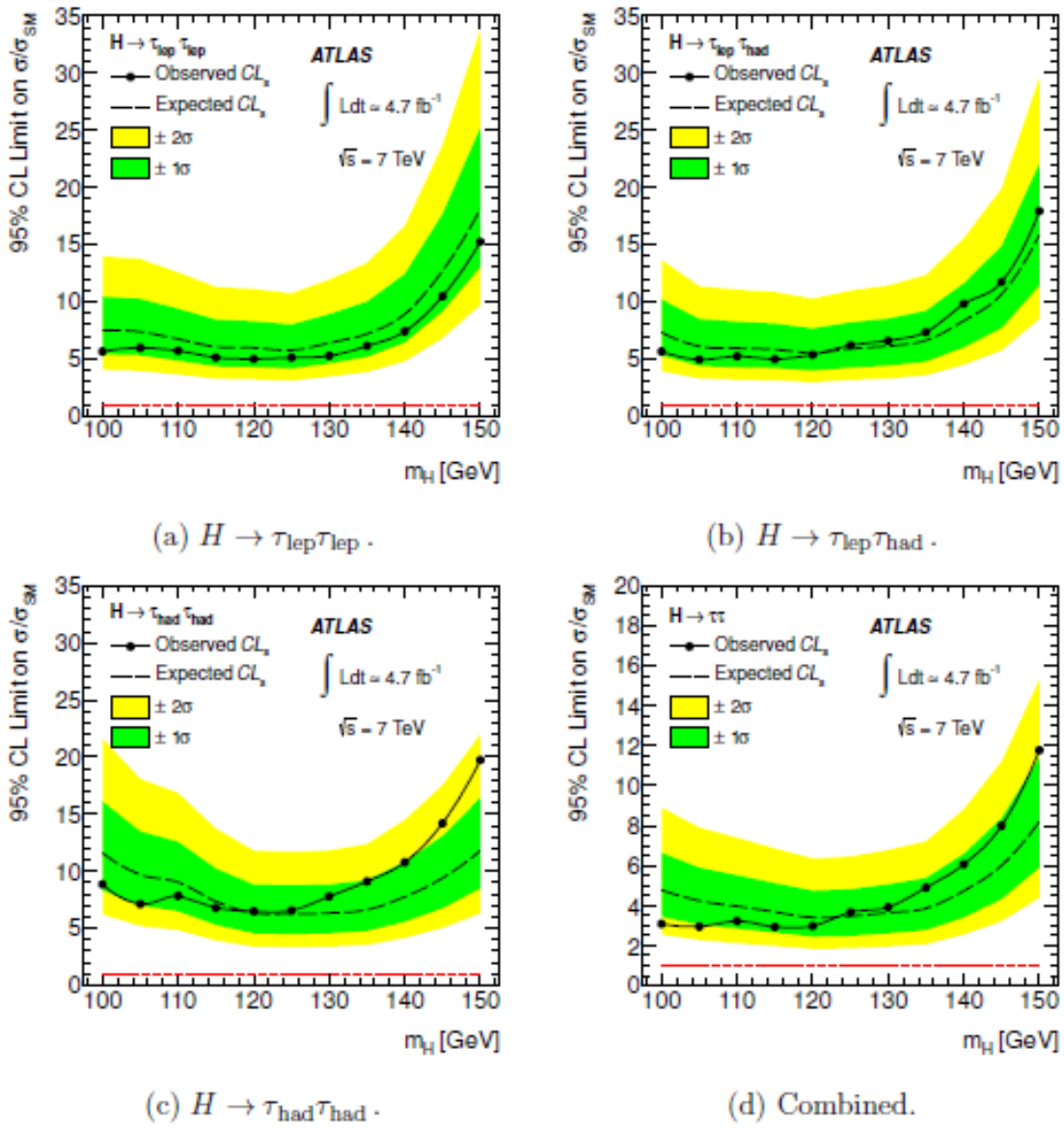

(a) $H \to \tau_{\mathrm{lep}}\tau_{\mathrm{lep}}$.

(b) $H \to \tau_{\mathrm{lep}}\tau_{\mathrm{had}}$.

(c) $H \to \tau_{\mathrm{had}}\tau_{\mathrm{had}}$.

(d) Combined.

Observed (solid) and expected (dashed) 95% confidence level upper limits on the Higgs boson cross section times branching ratio, normalised to the Standard Model expectation, as a function of the Higgs boson mass.

Search for supersymmetry in events with large missing transverse momentum, jets, and at least one tau lepton in 7 TeV proton-proton collision data with the ATLAS detector

Eur. Phys. J C.72 (2012) 2215

The ATLAS collaboration

A search for supersymmetry (SUSY) in events with large missing transverse momentum, jets, and at least one hadronically decaying τ lepton, with zero or one additional light lepton (e/μ), has been performed using 4.7 fb^{-1} of proton-proton collision data at $s\sqrt{=}7\sim\mathrm{TeV}$ recorded with the ATLAS detector at the Large Hadron Collider. No excess above the Standard Model background expectation is observed and a 95 % confidence level visible cross-section upper limit for new phenomena is set. In the framework of gauge-mediated SUSY-breaking models, lower limits on the mass scale Λ are set at 54 TeV in the regions where the $\tau\sim1$ is the next-to-lightest SUSY particle (tanβ>20). These limits provide the most stringent tests to date of GMSB models in a large part of the parameter space considered.

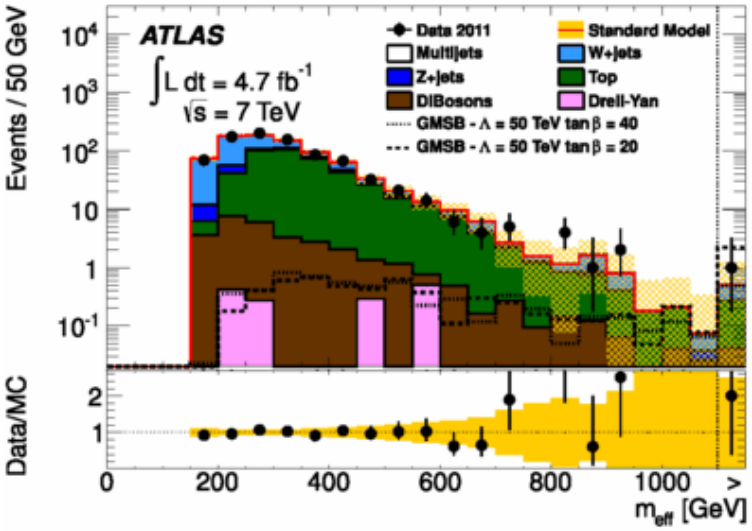

(a) m_{eff} distribution for the $\tau+\mu$ final state.

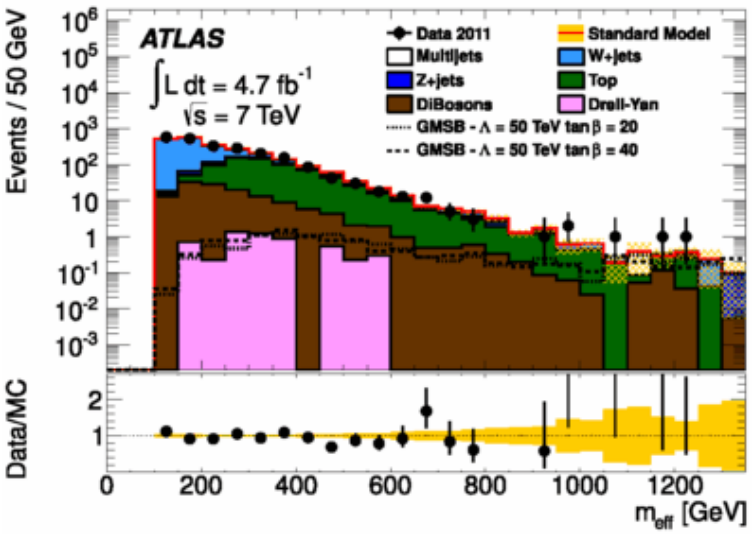

(b) m_{eff} distribution for the $\tau+e$ final state.

Distribution of m_{eff} for the (a) τ+μ and (b) τ+e final states after all analysis requirements. Data are represented by the points, with statistical uncertainty only. The SM prediction includes the data-driven corrections discussed in the text. The band centred around the total SM background indicates the uncertainty due to finite MC sample sizes on the background expectation. Also shown is the expected signal from two typical GMSB samples (Λ=50 TeV, tanβ=40, Λ=50 TeV, tanβ=20). In the top figure, the event in data surviving all the analysis requirements is shown in the overflow bin

Search for the Standard Model Higgs boson in the diphoton decay channel with 4.9 fb-1 of pp collisions at sqrt(s)=7 TeV with ATLAS

Phys. Rev. Lett. 108 (2012) 111803 DOI: http://dx.doi.org/10.1103/PhysRevLett.108.111803

The ATLAS collaboration

A search for the standard model Higgs boson is performed in the diphoton decay channel. The data used correspond to an integrated luminosity of 4.9 fb−1 collected with the ATLAS detector at the Large Hadron Collider in proton-proton collisions at a center-of-mass energy of $\sqrt{s}$=7 TeV. In the diphoton mass range 110–150 GeV, the largest excess with respect to the background-only hypothesis is observed at 126.5 GeV, with a local significance of 2.8 standard deviations. Taking the look-elsewhere effect into account in the range 110–150 GeV, this significance becomes 1.5 standard deviations. The standard model Higgs boson is excluded at 95% confidence level in the mass ranges of 113–115 GeV and 134.5–136 GeV.

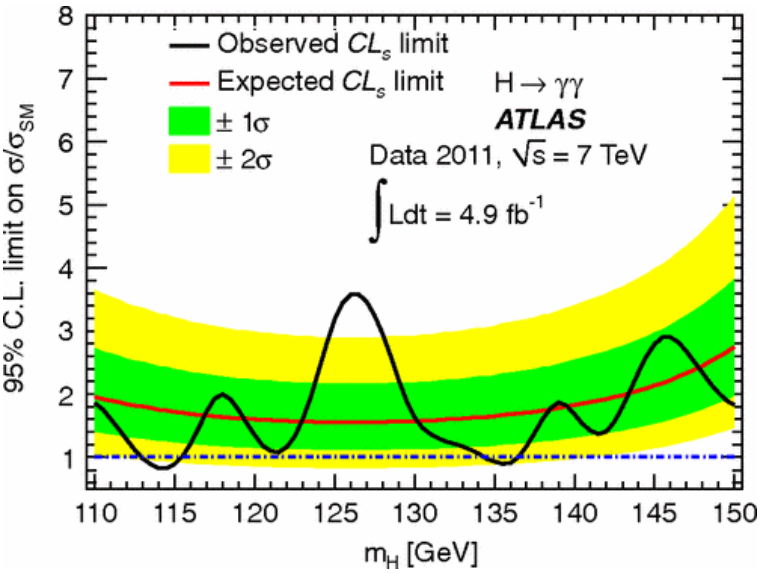

Observed and expected 95% C.L. limits on the SM Higgs boson production normalized to the predicted cross section as a function of m_H.

For Higgs masses below $135\mathrm{GeV}$, most of these Higgs bosons should decay into a pair of bottom quarks. However, because there are so many bottom quarks produced each second at the LHC, the bottom quark background would overwhelm the tiny signal associated with a Higgs boson. Instead, the rare event in which the Higgs bosons decay into two photons, with a probability of roughly one in five-hundred, is actually a better place to look for the Higgs boson. In the 2011 LHC data, fewer than 150 Higgs bosons should have decayed into photon pairs, but although there is a background of two-photon events, it is statistically manageable. What ATLAS has found in this paper is a potentially significant number of two-photon events, whose invariant mass clusters around $126\mathrm{GeV}$, above the expected background. (Although each photon is massless, the two-photon pair can collectively be assigned a mass value, called the invariant mass, that depends on the kinematical properties of the pair.) If the two photons originated from a decaying Higgs boson, their invariant mass can be identified with the mass of the decaying Higgs boson; that is, a Higgs mass of $126\mathrm{GeV}$.

Search for the neutral Higgs bosons of the Minimal Supersymmetric Standard Model in pp collisions at sqrt(s) = 7 TeV with the ATLAS detector

JHEP 02 (2013) 095

The ATLAS collaboration

A search for neutral Higgs bosons of the Minimal Supersymmetric Standard Model (MSSM) is reported. The analysis is based on a sample of proton-proton collisions at a centre-of-mass energy of 7 TeV recorded with the ATLAS detector at the Large Hadron Collider. The data were recorded in 2011 and correspond to an integrated luminosity of 4.7 fb^{-1} to 4.8 fb^{-1}. Higgs boson decays into oppositely-charged muon or τ lepton pairs are considered for final states requiring either the presence or absence of *b*-jets. No statistically significant excess over the expected background is observed and exclusion limits at the 95% confidence level are derived. The exclusion limits are for the production cross-section of a generic neutral Higgs boson, ϕ, as a function of the Higgs boson mass and for *h*/*A*/*H* production in the MSSM as a function of the parameters m_A and tan β in the TeX scenario for m_A in the range of 90 GeV to 500 GeV.

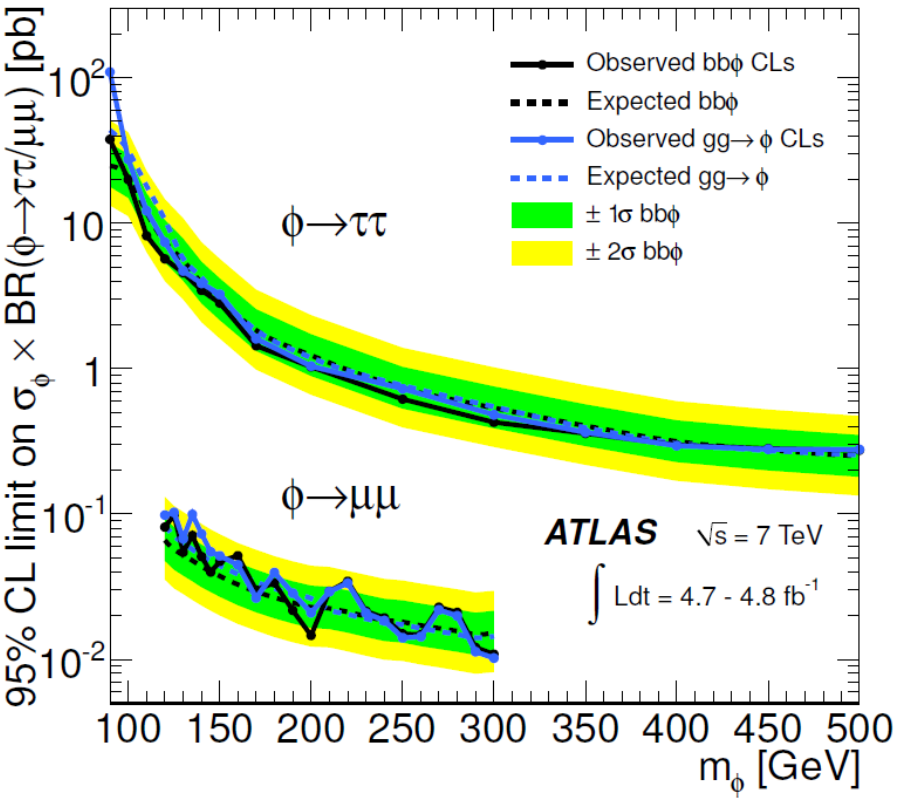

Expected (dashed line) and observed (solid line) 95% CL limits on the cross-section for gluon-fusion and b-associated Higgs boson production times the branching ratio into τ and μ pairs, respectively, along with the • }1 σ and • }2 σ bands for the expected limit. The combinations of all τ τ and μ μ channels are shown. The difference in the exclusion limits obtained for the gluon-fusion and the b-associated production modes is due to the different sensitivity from the b-tagged samples.

Higgs boson coupling sensitivity at the LHC using $H \to \tau\tau$ decays

Physics Review D 86, 073009 (2012) DOI: http://dx.doi.org/10.1103/PhysRevD.86.073009

Boddy, Farrington, Hays

We investigate the potential for measuring the relative couplings of a low-mass Higgs boson at the Large Hadron Collider using WH, ZH, and $t\bar{t}H$ production, where the Higgs boson decays to tau-lepton pairs. With 100 fb^{-1} of $\sqrt{s}$=14 TeV pp collision data we find that these modes can improve sensitivity to coupling-ratio measurements of a Higgs boson with a mass of about 125 GeV/c^2.

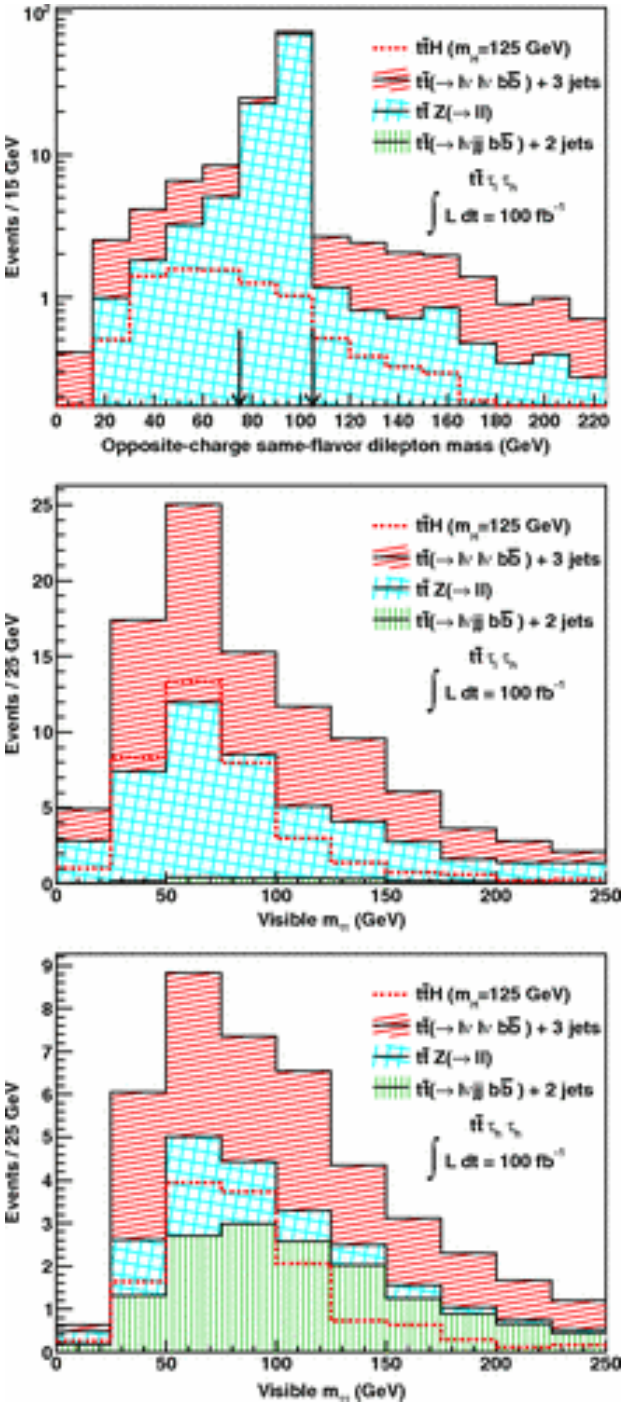

The $m(l_W\tau_l)$ (top), $m(\tau_h\tau_l)$ (middle), and $m(\tau_h\tau_h)$ distributions after all selection requirements [except for the requirement on $m(l_W\tau_l)$ for the $m(l_W\tau_l)$ distribution]. The selected $m(l_W\tau_l)$ regions are below and above the arrows in the $m(l_W\tau_l)$ plot. Shown are the $t\bar{t}H$ signal (dashed line) and the following backgrounds: $t\bar{t}$ +3 jets (tilted-lined region), $t\bar{t}$ +Z (tilted-hatched region), and $t\bar{t}$ +2 jets (vertical-lined region) production.

Measurement of the forward-backward asymmetry in the $B \to K^{(*)}\mu^+\mu^-$ Decay and First Observation of the $B^0_s \to \phi\mu^+\mu^-$ Decay

Phys. Rev. Lett. 106, 161801 (2011) DOI: http://dx.doi.org/10.1103/PhysRevLett.106.161801

The CDF collaboration incl. S. Farrington

We reconstruct the rare decays $B+ \to K+\mu+\mu-$, $B0 \to K*(892)0\mu+\mu-$, and $B0s \to \phi(1020)\mu+\mu-$ in a data sample corresponding to 4.4 fb−1 collected in pp^- collisions at $s\sqrt{}$=1.96 TeV by the CDF II detector at the Tevatron Collider. Using 121±16 $B+ \to K+\mu+\mu-$ and 101±12 $B0 \to K*0\mu+\mu-$ decays we report the branching ratios. In addition, we report the differential branching ratio and the muon forward-backward asymmetry in the $B+$ and $B0$ decay modes, and the $K*0$ longitudinal polarization fraction in the $B0$ decay mode with respect to the squared dimuon mass. These are consistent with the predictions, and most recent determinations from other experiments and of comparable accuracy. We also report the first observation of the $B0s \to \phi\mu+\mu-$ decay and measure its branching ratio BR($B0s \to \phi\mu+\mu-$)=[1.44±0.33±0.46]×10−6 using 27±6 signal events. This is currently the most rare $B0s$ decay observed.

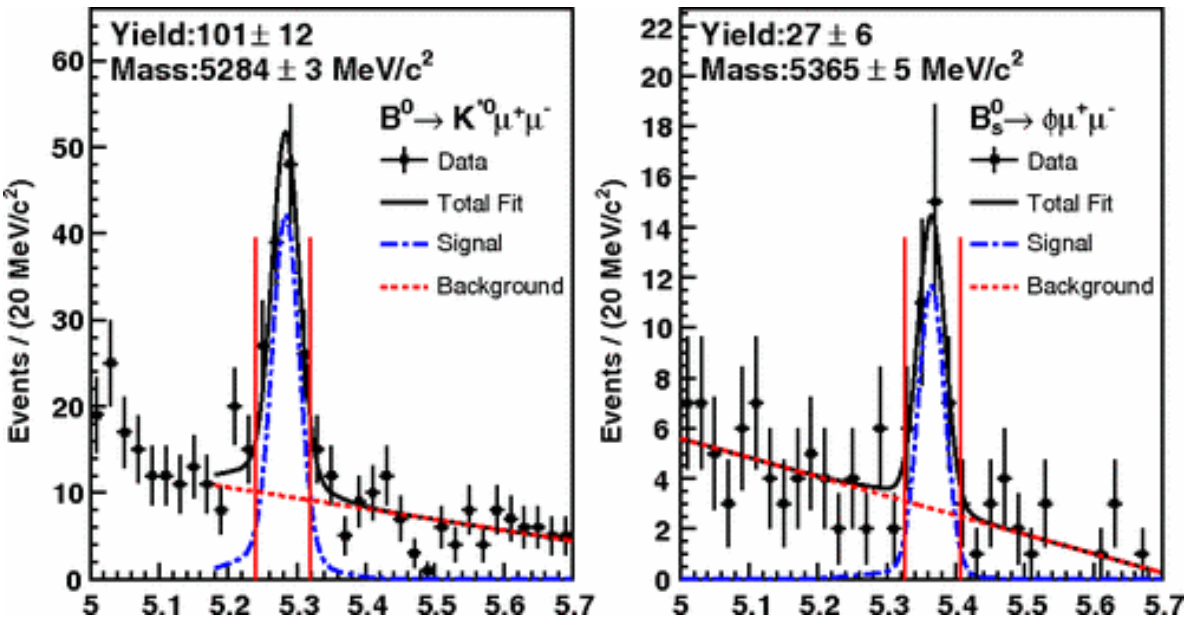

Mass of $B^0 \to K^{*0}\mu^+\mu^-$ and $B_s^0 \to \phi\mu^+\mu^-$ candidates with fit results overlaid. The vertical lines show the signal region

First Flavor-Tagged Determination of Bounds on Mixing-Induced CP Violation in Bs0 --> J/psi phi Decays

Phys. Rev. Lett. 100, 161802 (2008) DOI: http://dx.doi.org/10.1103/PhysRevLett.100.161802

CDF Collaboration incl. M. Kreps

This Letter describes the first determination of bounds on the *CP*-violation parameter $2\beta_s$ using $B0_s$ decays in which the flavor of the bottom meson at production is identified. The result is based on approximately 2000 $B0_s \to J/\psi\phi$ decays reconstructed in a 1.35 fb−1 data sample collected with the CDF II detector using pp^- collisions produced at the Fermilab Tevatron. We report confidence regions in the two-dimensional space of $2\beta_s$ and the decay-width difference $\Delta\Gamma$. Assuming the standard model predictions of $2\beta_s$ and $\Delta\Gamma$, the probability of a deviation as large as the level of the observed data is 15%, corresponding to 1.5 Gaussian standard deviations.

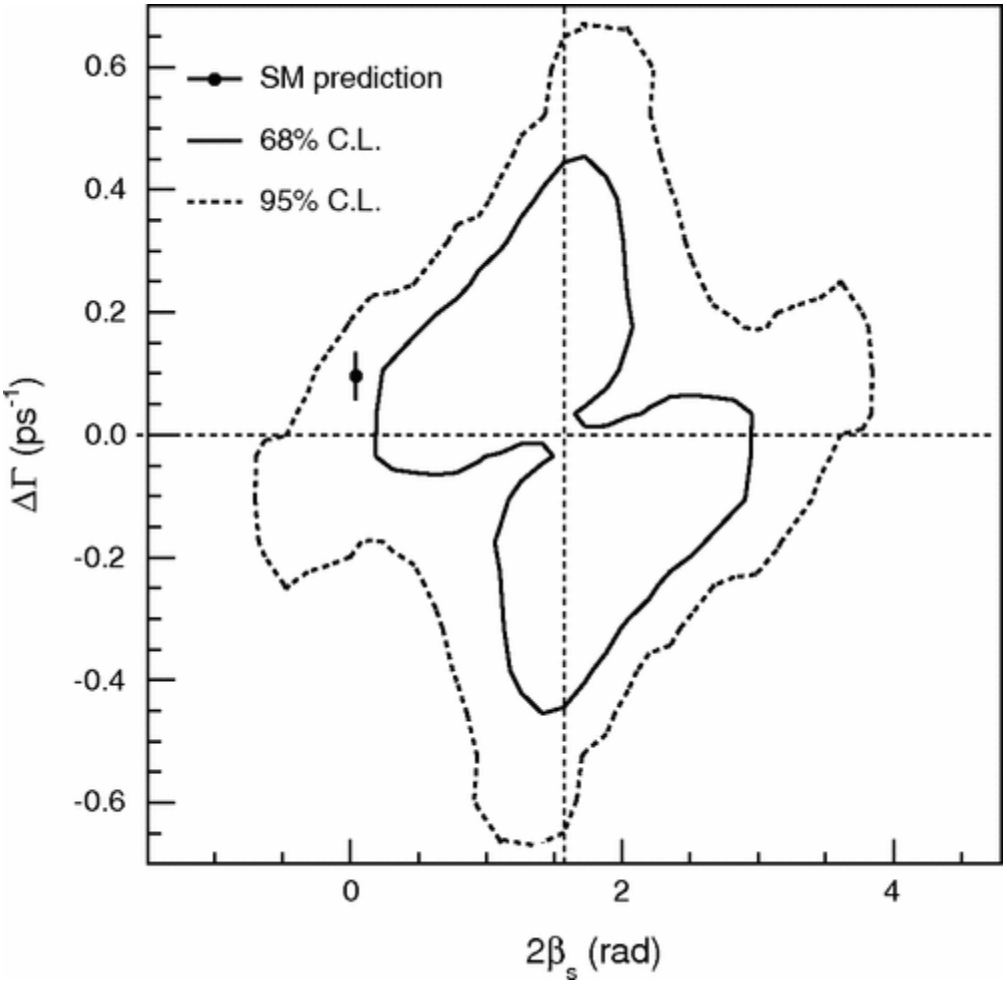

Feldman-Cousins confidence region in the $2\beta_s$-$\Delta\Gamma$ plane, where the standard model favored point is shown with error bars [9]. The intersection of the horizontal and vertical dotted lines indicates the reflection symmetry in the $2\beta_s$-$\Delta\Gamma$ plane

Measurement of Lifetime and Decay-Width Difference in Bs0 --> J/psi phi Decays

Phys. Rev. Lett. 100, 121803 (2008) DOI: http://dx.doi.org/10.1103/PhysRevLett.100.121803

CDF Collaboration incl. M. Kreps

We measure the mean lifetime $\tau=2/(\Gamma L+\Gamma H)$ and the decay-width difference $\Delta\Gamma=\Gamma L-\Gamma H$ of the light and heavy mass eigenstates of the $B0s$ meson, $B0sL$ and $B0sH$, in $B0s\rightarrow J/\psi\phi$ decays using 1.7 fb−1 of data collected with the CDF II detector at the Fermilab Tevatron pp^- collider. Assuming CP conservation, a good approximation for the $B0s$ system in the standard model, we obtain $\Delta\Gamma=0.076+0.059-0.063(\text{stat})\pm0.006(\text{syst})$ ps−1 and $\tau=1.52\pm0.04(\text{stat})\pm0.02(\text{syst})$ ps, the most precise measurements to date. Our constraints on the weak phase and $\Delta\Gamma$ are consistent with CP conservation.

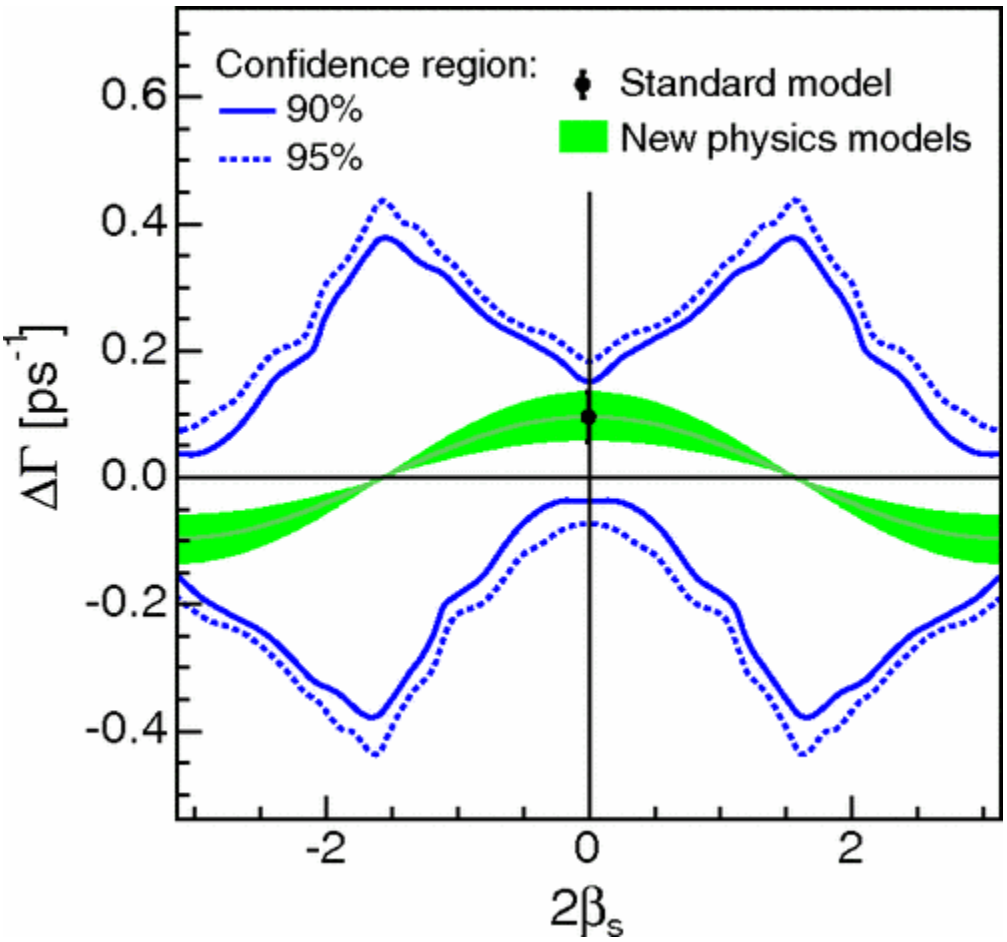

Regions at the 90% and 95% confidence level in the $2\beta_s$-$\Delta\Gamma$ plane compared with the SM prediction and the region allowed in new physics models given by $\Delta\Gamma=2|\Gamma_{12}|\cos(\phi_s)$

Precision Measurement of the X(3872) Mass in J/psi pi+ pi- Decays

Phys. Rev. Lett. 103, 152001 (2009) DOI: http://dx.doi.org/10.1103/PhysRevLett.103.152001

CDF Collaboration incl. M. Kreps

We present an analysis of the mass of the $X(3872)$ reconstructed via its decay to $J/\psi\pi+\pi-$ using 2.4 fb−1 of integrated luminosity from pp^{-} collisions at $s\sqrt{}=1.96$ TeV, collected with the CDF II detector at the Fermilab Tevatron. The possible existence of two nearby mass states is investigated. Within the limits of our experimental resolution the data are consistent with a single state, and having no evidence for two states we set upper limits on the mass difference between two hypothetical states for different assumed ratios of contributions to the observed peak. For equal contributions, the 95% confidence level upper limit on the mass difference is 3.6 MeV/c2. Under the single-state model the $X(3872)$ mass is measured to be 3871.61±0.16(stat)±0.19(syst) MeV/c2, which is the most precise determination to date.

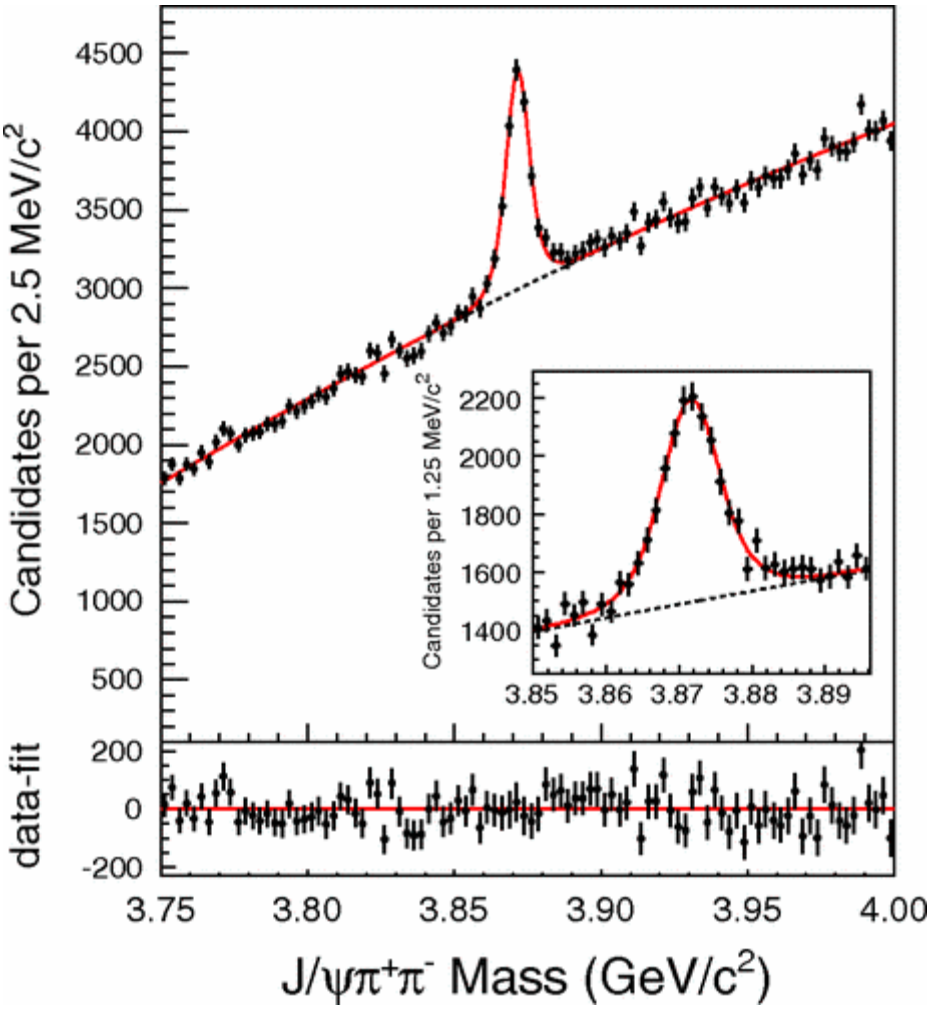

Invariant mass distribution of the $X(3872)$ candidates. The points show the data distribution, the full line is the projection of the unbinned maximum-likelihood fit, and the dashed line corresponds to the background part of the fit. The inset shows an enlargement of the region around the $X(3872)$ peak. Residuals of the data with respect to the fit are displayed below the mass plot.

Measurement of the CP-violating phase $\beta_{J/\psi\phi s}$ in $B0s \to J/\psi\phi$ decays with the CDF II detector

Phys. Rev. D 85, 072002 (2012) DOI: http://dx.doi.org/10.1103/PhysRevD.85.072002

CDF Collaboration incl. M. Kreps

We present a measurement of the CP-violating parameter $\beta J/\psi\phi s$ using approximately 6500 $B0s \to J/\psi\phi$ decays reconstructed with the CDF II detector in a sample of pp^{-} collisions at $s\sqrt{}=1.96$ TeV corresponding to 5.2 fb-1 integrated luminosity produced by the Tevatron collider at Fermilab. We find the CP-violating phase to be within the range $\beta J/\psi\phi s \in [0.02,0.52] \cup [1.08,1.55]$ at 68% confidence level where the coverage property of the quoted interval is guaranteed using a frequentist statistical analysis. This result is in agreement with the standard model expectation at the level of about one Gaussian standard deviation. We consider the inclusion of a potential S-wave contribution to the $B0s \to J/\psi K+K-$ final state which is found to be negligible over the mass interval $1.009<m(K+K-)<1.028$ GeV/$c2$. Assuming the standard model prediction for the CP-violating phase $\beta J/\psi\phi s$, we find the $B0s$ decay width difference to be $\Delta\Gamma s=0.075\pm0.035(\text{stat})\pm0.006(\text{syst})$ ps-1. We also present the most precise measurements of the $B0s$ mean lifetime $\tau(B0s)=1.529\pm0.025(\text{stat})\pm0.012(\text{syst})$ ps, the polarization fractions $|A0(0)|2=0.524\pm0.013(\text{stat})\pm0.015(\text{syst})$ and $|A\|(0)|2=0.231\pm0.014(\text{stat})\pm0.015(\text{syst})$, as well as the strong phase $\delta\perp=2.95\pm0.64(\text{stat})\pm0.07(\text{syst})$ rad. In addition, we report an alternative Bayesian analysis that gives results consistent with the frequentist approach.

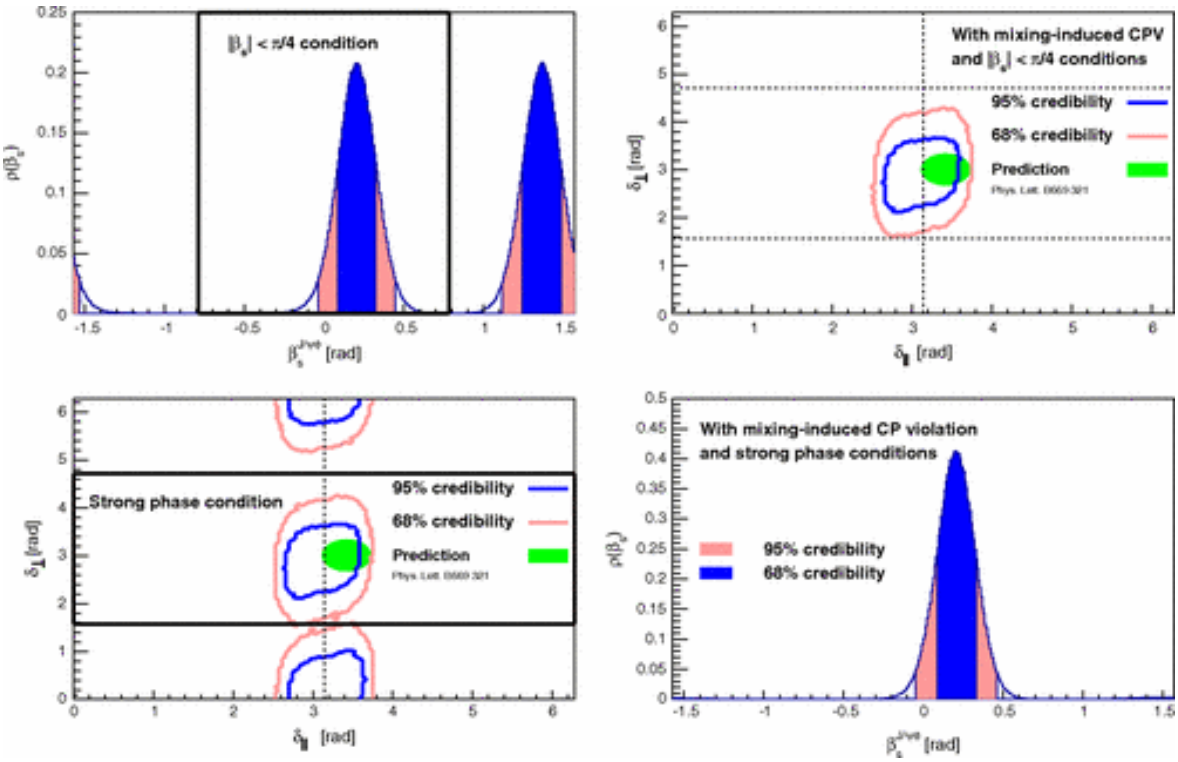

Conditional posterior densities for $\delta_\perp$ versus $\delta_\parallel$ and for $\beta_s^{J/\psi\phi}$. The extra conditions applied to $\beta_s^{J/\psi\phi}$ (top row) and $\delta_\perp$ (bottom row) are shown on the left, and the resulting conditional probabilities are displayed on the right. The theoretical prediction of Ref. 63 is indicated as green ellipse in the bottom left plot. All plots in this figure are subject to the constraint of mixing-induced CP violation. The dark-solid (blue) and light-solid (red) contours show the 68% and 95% credible regions, respectively.